BBA - Molecular Basis of Disease 1865 (2019) 2094–2110

Contents lists available at ScienceDirect

BBA - Molecular Basis of Disease

journal homepage: www.elsevier.com/locate/bbadis

The metastasis suppressor, NDRG1, differentially modulates the endoplasmic reticulum stress response

A.M. Merlot[a,b,*], G.M. Porter[a,b], S. Sahni[b], E.G. Lim[b], P. Peres[b], D.R. Richardson[b,c,**]

[a] Cancer Targets and Therapeutics Group, Lowy Cancer Research Centre, UNSW Centre for Childhood Cancer Research (C25), Faculty of Medicine, The University of New South Wales, Kensington, New South Wales 2031, Australia

[b] Molecular Pharmacology and Pathology Program, Discipline of Pathology and Bosch Institute, Medical Foundation Building (K25), The University of Sydney, Sydney, New South Wales 2006, Australia

[c] Department of Pathology and Biological Responses, Nagoya University Graduate School of Medicine, 65 Tsurumai, Showa-ku, Nagoya 466-8550, Japan

ARTICLE INFO

Keywords:
NDRG1
Endoplasmic reticulum
Unfolded protein response
Thiosemicarbazones

ABSTRACT

The metastasis suppressor, N-myc downstream regulated gene-1 (NDRG1), is a stress response protein that is involved in the inhibition of multiple oncogenic signaling pathways. Initial studies have linked NDRG1 and the endoplasmic reticulum (ER) stress response. Considering this, we extensively examined the mechanism by which NDRG1 regulates the ER stress response in pancreatic and colon cancer cells. We also examined the anti-cancer agent, di-2-pyridylketone 4,4-dimethyl-3-thiosemicarbazone (Dp44mT), which induces NDRG1 expression and causes ER stress. The expression of NDRG1 was demonstrated to regulate the three main arms of the ER stress response by: (1) increasing the expression of three major ER chaperones, binding immunoglobulin protein (BiP), calreticulin, and calnexin; (2) suppressing the protein kinase, RNA-activated (PKR)-like ER kinase (PERK); (3) inhibiting the inositol-requiring kinase 1α (IRE1α) arm; and (4) increasing the cleavage of activating transcription factor 6 (ATF6). An important finding was that NDRG1 enhances the anti-proliferative and anti-migratory activity of Dp44mT. This increased efficacy could be related to the following effects in the presence of Dp44mT and NDRG1, namely: markedly increased activation of the PERK target, eukaryotic translation initiation factor 2α (eIF2α); the maintenance of activating transcription factor 4 (ATF4) expression; high cytosolic Ca^{+2} that increases the sensitivity of cells to apoptosis *via* activation of the calmodulin-dependent kinase II (CaMKII) signaling cascade; and increased pro-apoptotic C/EBP-homologous protein (CHOP) expression. Collectively, this investigation dissects the molecular mechanisms through which NDRG1 manipulates the ER stress response and its ability to potentiate the activity of the potent anti-cancer agent, Dp44mT.

1. Introduction

The endoplasmic reticulum (ER) is a critical organelle responsible for the synthesis, post-translational modification and folding of proteins, calcium (Ca^{+2}) homeostasis and lipid biosynthesis in eukaryotic cells [1–3]. The ER is highly sensitive to changes in the cellular environment, including hypoxia, glucose-deprivation, oxidative stress, acidosis, high adipose, and cholesterol, with these various insults disrupting protein-folding to induce ER stress [1–4]. Following ER stress, cells activate a series of homeostatic signaling networks to cope with protein-folding alterations, known as the unfolded protein response (UPR) [1–4]. The UPR relays information about the protein-folding status of the ER to the nucleus and cytosol to buffer variations and restore homeostasis [1–4].

The UPR consists of dynamic signaling pathways initiated by three main ER trans-membrane proteins: (1) protein kinase, RNA-activated

Abbreviations: ATF6, activating transcription factor 6; BiP, binding immunoglobulin protein; CaMKII, calmodulin-dependent kinase II; CHOP, C/EBP-homologous protein; DFO, desferrioxamine; Dp2mT, di-2-pyridylketone 2-methyl-3-thiosemicarbazone; Dp44mT, di-2-pyridylketone 4,4-dimethyl-3-thiosemicarbazone; DpT, di-2-pyridylketone thiosemicarbazone; eIF2α, eukaryotic translation initiation factor 2; ER, endoplasmic reticulum; ERAD, ER-associated degradation; HIF-1α, hypoxia-inducible factor-1α; IRE1α, inositol-requiring kinase 1α; JNK, c-jun *N*-terminal kinase; NDRG1, N-myc downstream regulated gene-1; PERK, RNA-activated (PKR)-like ER kinase; UPR, unfolded protein response; XBP1, X-box binding protein-1

* Correspondence to: A.M. Merlot, Lowy Cancer Research Centre, The University of New South Wales, C25/9 High St, Kensington, New South Wales 2031, Australia.

** Correspondence to: D.R. Richardson, Discipline of Pathology and Bosch Institute, The University of Sydney, Sydney, New South Wales 2006, Australia.

E-mail addresses: a.merlot@unsw.edu.au (A.M. Merlot), d.richardson@sydney.edu.au (D.R. Richardson).

https://doi.org/10.1016/j.bbadis.2019.04.007
Received 12 February 2019; Received in revised form 2 April 2019; Accepted 9 April 2019
Available online 11 April 2019

(PKR)-like ER kinase (PERK); (2) inositol-requiring kinase 1α (IRE1α); and (3) activating transcription factor 6 (ATF6) [1–3]. In the absence of ER stress, binding immunoglobulin protein (BiP) binds to the luminal domains of PERK, IRE1α and ATF6, rendering them inactive [5,6]. In response to ER stress, BiP preferentially binds to misfolded/unfolded proteins in the ER and dissociates from PERK, IRE1α and ATF6, resulting in the activation of these transducers and their subsequent downstream signaling networks [5,6]. Together, PERK, IRE1α and ATF6 control the expression of various overlapping genes that reduce ER protein mis-folding, and promote cell survival [1–3]. In conditions of persistent and intense cellular stress, these adaptive and cytoprotective responses switch to pro-apoptotic signaling [1–3].

Upon activation by phosphorylation, PERK phosphorylates eukaryotic translation initiation factor-2α (eIF2α), resulting in the inhibition of general protein synthesis [1,7]. Subsequently, p-eIF2α paradoxically promotes the selective translation of activating transcription factor-4 (*ATF4*) mRNA [1,7]. Then, ATF4 activates UPR target genes, which control the transcription of genes involved in autophagy, apoptosis and amino acid metabolism [1,7]. For instance, ATF4 can up-regulate the pro-apoptotic transcription factor, C/EBP-homologous protein (CHOP), inducing apoptosis [6,8]. During ER stress, dimerization and auto-phosphorylation of IRE1α results in alternate X-box binding protein-1 (*XBP1*) mRNA splicing to generate XBP1s [9]. XBP1s is a pro-survival transcription factor that controls the expression of genes involved in protein-folding and ER-associated degradation (ERAD), such as BiP and $p58^{IPK}$ [9]. However, under chronic stress, p-IRE1α can also activate c-jun *N*-terminal kinase (JNK), which induces apoptosis [9]. The third axis of the UPR is initiated by ATF6 activation, where ATF6 is transported to the Golgi and cleaved [6]. Cleaved ATF6 undergoes nuclear translocation to control the transcription of genes encoding proteins required for ERAD, ER and Golgi biogenesis, as well as ER proteins and chaperones (*e.g.*, XBP1, BiP, *etc.*) [8,9].

The pro-survival activation of the UPR has been demonstrated in several cancer-types and is implicated in tumorigenesis [10–12]. Molecules in all three pathways of the UPR show altered expression patterns across multiple tumors, including colon, liver, pancreatic and prostate cancer [13–19]. The highly proliferative nature of tumors necessitates an elevation in protein synthesis and enhances the metabolic burden on the ER and thereby activates the UPR [10]. Moreover, cancer cells are frequently subjected to a stressful microenvironment due to their highly proliferative nature and the lack of adequate blood supply for this expansion, resulting in hypoxia, acidosis and nutrient deprivation [20]. These environmental factors disrupt ER protein-folding and induce ER stress, thereby activating the UPR in an attempt to survive and adapt [10,21]. Depending on the cellular context, UPR activation in cancer cells stimulates adaptation, survival, angiogenesis and tumor growth [10,11]. Moreover, the UPR can stimulate cellular senescence, inducing dormancy of cancer cells until more favourable conditions occur [10–12].

N-myc downstream regulated gene 1 (NDRG1) is a stress response protein that is down-regulated in certain cancer-types, and this down-regulation correlates with poorly differentiated, advanced cancers [22–24]. In fact, NDRG1 is a metastasis suppressor in a number of cancer-types, including pancreatic, prostate, colon and breast [22–27]. Various factors up-regulate NDRG1, for instance, hypoxia, DNA damage and iron depletion [28,29]. Pharmacological agents that bind iron markedly up-regulate NDRG1, *via* their ability to induce hypoxia-inducible factor-1α (HIF-1α)-dependent and independent mechanisms [30–33]. These compounds have been developed as potent, clinically-trialled, anti-cancer agents and are known as the di-2-pyridylketone thiosemicarbazones (DpTs) that include di-2-pyridylketone 4,4-dimethyl-3-thiosemicarbazone (Dp44mT; Fig. 1A), which binds metal ions and generates redox stress [33–39].

It was suggested that NDRG1 plays a role in the ER stress response [40]. Over-expression of NDRG1 suppresses stress-induced autophagy through the attenuation of the PERK-eIF2α pathway of the UPR, which induces apoptosis [40]. These findings indicate that NDRG1-mediated suppression of the pro-survival autophagic pathway could play a role in its anti-metastatic effects by inducing apoptosis [40]. As such, there is a link between NDRG1 and the ER stress response. While these initial results are promising, the molecular mechanism by which NDRG1 regulates the ER stress response is unknown and was the aim of this study examining pancreatic cancer and colon cancer cells. We hypothesize that NDRG1 not only regulates the PERK pathway, but regulates all three main arms of the ER stress response. To investigate this, studies utilized NDRG1 over-expressing cells, NDRG1 silenced cells and the NDRG1-inducing agent, Dp44mT. This investigation demonstrates NDRG1 expression regulates all three arms of the ER stress response and enhances the anti-proliferative activity of Dp44mT and its ability to inhibit tumor cell migration.

2. Materials and methods

2.1. Chemicals

The thiosemicarbazone, Dp44mT, and its negative control, di-2-pyridylketone 2-methyl-3-thiosemicarbazone (Dp2mT; Fig. 1A), were synthesized and characterized using standard methods [38]. Desferrioxamine (DFO; Fig. 1A) was purchased from Sigma-Aldrich (St. Louis, MO). Both Dp44mT and Dp2mT were dissolved in dimethyl sulfoxide (DMSO) and diluted in media to produce a 10 μM solution with a final DMSO concentration being < 0.5% (v/v). This DMSO concentration had no effect on cellular proliferation [41]. DFO was dissolved directly in media to a final concentration of 250 μM. All solutions were prepared immediately prior to each experiment.

2.2. Cell culture

The human pancreatic cancer cell line, PANC1, and the human colon cancer cell line, HT-29, were purchased from the American Type Culture Collection (ATCC; Manassas, VA). PANC1 and HT-29 cells were cultured in Dulbecco's Modified Eagle Medium (DMEM; Sigma-Aldrich) and McCoy's 5A medium, respectively, at 37 °C in an atmosphere of 5% CO_2/95% air. This media was supplemented with 10% (v/v) fetal calf serum (FCS; Sigma-Aldrich) and the following additives from Sigma-Aldrich: 1% (v/v) sodium pyruvate, 1% (v/v) non-essential amino acids, 100 U/mL penicillin, 100 μg/mL streptomycin, 2 mM glutamine and 0.28 μg/mL Fungizone.

2.3. Plasmid construction and transfection

NDRG1 over-expressing and vector control PANC1 or HT-29 cells were generated using the pCMV-tag2-FLAG-NDRG1 vector (GenHunter, Nashville, TN, USA) and the empty pCMV-tag2-FLAG vector (Stratagene, Santa Clara, CA, USA), respectively [42,43]. Both plasmids possess a G418 resistance marker and were developed using established techniques [42,43]. NDRG1 over-expression and control transfections were selected and maintained with G418 (0.3 mg/mL; Alexis Biochemicals, CA, USA). Cells were transfected as described previously using Lipofectamine 2000 (Life Technologies, VIC, Australia).

2.4. Western blot analysis

Western blot analysis was performed as described previously [34]. The primary antibodies used include: IRE1α (1:1000, Cat. #3294), BiP (1:1000, Cat. #3177), PERK (1:1000, Cat. #3192), eIF2α (1:1000, Cat. #5324), XBP1 (1:100, Cat. #12782), $p58^{IPK}$ (1:1000, Cat. #2940), CHOP (1:1000, Cat. #2895), ATF4 (1: 1000, Cat. #11815), JNK (1:1000, Cat. #9252S), p-JNK (1:1000, Cat. #9251S), CAMKII (1:1000, Cat. #3362), p-CAMKII (1:1000, Cat. #12716), calnexin (1:1000, Cat. #2679), calreticulin (1:1000, Cat. #2891) and p-eIF2α (1:1000, Cat. #3398) from Cell Signaling Technology (MA, USA). Primary antibodies

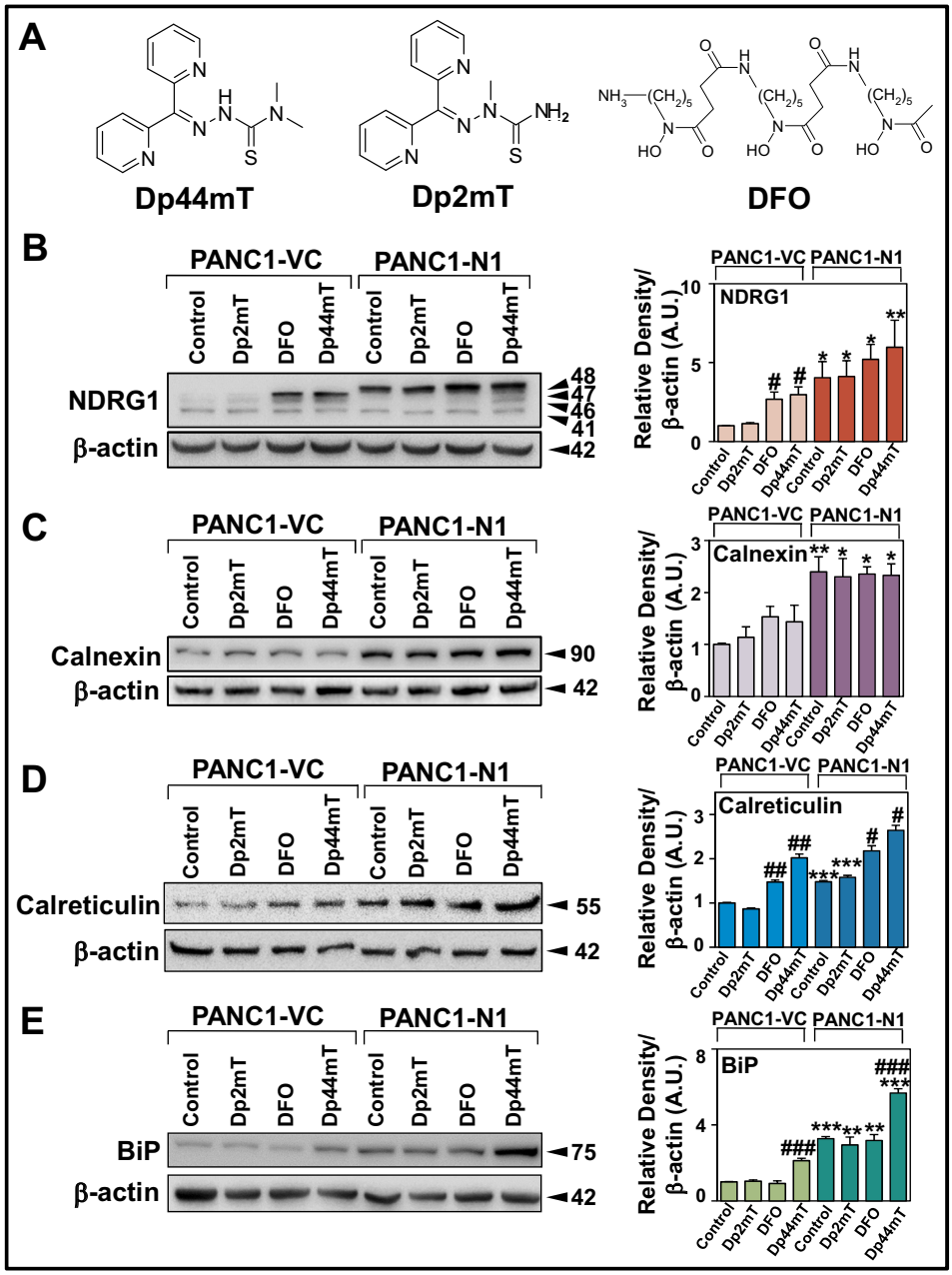

Fig. 1. Expression of NDRG1 and endoplasmic reticulum (ER) chaperones, calnexin, calreticulin and binding immunoglobulin protein (BiP), in PANC1-VC and PANC1-N1 cells following incubation with either Dp2mT, DFO or Dp44mT. (A) Line drawings of the chemical structures of the agents: di-2-pyridylketone-4,4,-dimethyl-3-thiosemicarbazone (Dp44mT), di-2-pyridylketone 2-methyl-3-thiosemicarbazone (Dp2mT) and desferrioxamine (DFO). (B–E) Pancreatic cancer cells transfected with an empty vector (PANC1-VC) or an NDRG1-expressing vector (PANC1-N1) were incubated with control media or media containing Dp2mT (10 μM), DFO (250 μM) and Dp44mT (10 μM) for 24 h/37 °C. (B) NDRG1, (C) calnexin, (D) calreticulin and (E) BiP expression was analyzed in PANC1-VC and PANC1-N1 cells. Results are typical of at least three experiments and the densitometric analysis is represented as mean ± SEM (3 experiments) normalized to β-actin (arbitrary units; A.U.). $^{\#}p < 0.05$, $^{\#\#}p < 0.01$, $^{\#\#\#}p < 0.001$; relative to respective controls $^{*}p < 0.05$, $^{**}p < 0.01$, $^{***}p < 0.001$; relative to their corresponding treatments in PANC1-VC cells.

against NDRG1 (1:2000, Cat. #ab37897) and p-IRE1α (1:1000, Cat. #ab124945) were from Abcam (Cambridge, UK). A primary antibody against p-PERK (1:1000, Cat. #649402) was purchased from BioLegend (San Diego, CA), while a primary antibody against ATF6 (1:1000, Cat. #IMG-127) was from Santa Cruz (Santa Cruz, CA). The primary antibody against β-actin (1:10000, Cat. #A1978) was purchased from Sigma-Aldrich, while horseradish peroxidase (HRP)-conjugated anti-rabbit IgG, anti-mouse IgG and anti-goat IgG (1:10,000; Sigma-Aldrich) were used as secondary antibodies. Enhanced chemiluminescence (ECL) Plus™ Western Blotting Detection Reagents (GE Healthcare, Australia) were implemented for detection and images were captured using a ChemiDoc™ MP Imaging System (Bio-Rad, Hercules, CA).

2.5. Densitometric analysis

Densitometric analysis of western blots was carried out using ChemiDoc Image Lab Software (BioRad). The densitometry represents the total bands detected when multiple bands were evident for a protein, unless specified. Data was normalized using the corresponding β-actin loading controls.

2.6. Confocal microscopy

PANC1-VC and PANC1-N1 cells (1×10^5 cells/mL) were grown overnight on cover slips to 70% confluency. Cells were subsequently incubated with Dp44mT (10 μM) or control media for 24 h/37 °C. Following incubation, cells were fixed with ice-cold methanol for 10 min at room temperature. Cells were subsequently washed with PBS (3 × 5 min) and permeabilized with Triton X-100 (0.2%/5 min). After further washing cells in PBS and blocking non-specific binding with 5% BSA/PBS (30 min, pH 7.5), immunocytochemistry was performed with rabbit monoclonal anti-NDRG1 (Cat. #9485, Cell Signaling Technology), mouse monoclonal anti-GRP78 BiP (Cat. #Ab181499, Abcam), mouse monoclonal anti-calreticulin (Cat. #ab22683), rabbit monoclonal anti-calnexin C5C9 (Cat. #2679T, Cell Signaling Technology) and Alexa Fluor-conjugated secondary antibodies (Life

Technologies, Carlsbad, CA). Cover slips were mounted on slides using the ProLong Gold DAPI (4′,6-diamidino-2-phenylindole) anti-fade mounting solution (Life Technologies). Slides were examined with a Zeiss LSM 510 Meta confocal microscope (Zeiss, Oberkochen, Germany) equipped with FITC and Texas Red filters. Fluorescence intensity and the Mander's (M2) coefficient for co-localization (r) were measured using ImageJ 4.7v software (National Institutes of Health, Baltimore, MD).

2.7. Measurement of intracellular Ca^{+2}

Fura-2 AM (acetoxymethyl; Sigma–Aldrich), a fluorescent Ca^{+2} indicator, was used to detect intracellular Ca^{+2} levels according to the manufacturer's protocol using Ca^{+2}-free media (Cat. #: 21068028; Life Technologies) under established conditions [34]. Briefly, PANC1-VC and PANC1-N1 cells were incubated in the presence or absence of Dp2mT (10 μM), DFO (250 μM), or Dp44mT (10 μM) for 24 h/37 °C. The cells were subsequently loaded with 2 μM Fura-2 AM in media for 30 min/37 °C in the dark, washed and further incubated in Ca^{+2}-free media to allow complete de-esterification of intracellular AM esters. After incubation, cells were washed in a Ca^{+2}-free Tyrodes salt solution. Fluorescence was measured with the emission signal detected at 510 nm and excitation at 340 and 380 nm using a CLARIOStar Microplate Reader (BMG LABTECH, Germany). Intracellular Ca^{+2} concentrations were calculated, as described previously [34,44].

2.8. Gene silencing by small interfering RNA

PANC1-VC cells were grown to 40% confluency prior to siRNA transfection. Cells were transfected with SignalSilence *PERK* siRNA I (Cat. #9024, Cell Signaling Technology), *IRE1α* siRNA (Cat. #s200430, Ambion, CA, USA), *ATF6* siRNA (Cat. #EHU015441, Sigma-Aldrich), *NDRG1* siRNA (Cat. #s20336, Life Technologies) or SignalSilence Control siRNA (Cat. #6568, Cell Signaling Technology) using Lipofectamine® 2000 Reagent in Opti-MEM I Reduced Serum Medium (Life Technologies), as per the manufacturer's protocol [34].

2.9. Cellular proliferation assay

Cellular proliferation was assessed as performed previously [41], using the MTT [3-(4, 5-dimethylthiazol-2-yl)-5-(3-carboxymethoxyphenyl)-2-(4-sulfophenyl)-2H-tetrazolium] assay. PANC1-VC and PANC1-N1 cells were seeded into 96 well plates at a density of 7000 cells/well and incubated overnight at 37 °C in a 5% CO_2 atmosphere. Following this incubation, cells were incubated with Dp44mT (0–10 μM) or control media for 48 h/37 °C. Subsequently, 10 μL of MTT solution (5 mg/mL in PBS, Sigma-Aldrich) was added to each well and incubated for 2 h/37 °C. Cells were then lyzed using 100 μL of DMSO for 10 min/37 °C. The absorbance was measured at 570 nm by the Victor TM Multi-label Counter plate reader (Perkin Elmer, VIC, Australia) and is representative of the number of viable cells. Results were expressed as the concentration required to inhibit growth by 50% (IC_{50}). Validation of MTT proliferation results was performed *via* viable cell counts using Trypan blue [41].

2.10. Real-time cell analyzer (RTCA) migration assay

RTCA Migration Assays were performed following the manufacturer's protocol (Roche Applied Science, Penzberg, Germany). Transfected PANC1-VC and PANC1-N1 cells were incubated with or without Dp44mT (24 h/37 °C) and subsequently resuspended in serum-free DMEM. Cell viability was assessed using Trypan blue solution and found to be > 90%, with the cells then being seeded in RTCA Cim-16 plates (xCELLigence, Roche) in the absence of Dp44mT. Complete DMEM with 10% FCS was added to the lower chamber as a chemoattractant. Measurements of real-time cell index (CI) were taken periodically over 48 h/37 °C using an xCELLigence RTCA Dual-Plate (DP) instrument (Roche Applied Science). CI is a relative change in measured electrical impedance derived by the xCELLigence RTCA DP instrument and was used to represent migration propensity.

2.11. Statistical analysis

Data was expressed as mean ± standard error of the mean (S.E.M.) of at least 3 independent experiments and was normalized to the control of the relevant vector control cell-type. Statistical analysis was performed using Student's t-test and results were considered significant when $p < 0.05$.

3. Results

3.1. DFO and Dp44mT up-regulate NDRG1 expression

NDRG1 has previously been linked to the ER stress response and the UPR [40]. However, the nature and extent of the interaction of NDRG1 with these later processes is yet to be elucidated, particularly regarding the molecular mechanisms involved. To determine the effects of NDRG1 on the expression of key proteins associated with ER stress and the UPR, we initially utilized PANC1 pancreatic cancer cells over-expressing NDRG1 (PANC1-N1) cells relative to PANC1 cells transfected with the empty vector (PANC1-VC).

To assess the effect of NDRG1 on ER stress, PANC1-VC and PANC1-N1 cells were incubated for 24 h/37 °C with either media alone, or media containing Dp44mT (10 μM; Fig. 1A), which can induce both NDRG1 [30,40] and ER stress *via* metal sequestration and/or redox activity [35–38]. The relevant controls for Dp44mT included: (1) the Dp44mT analogue, Dp2mT (10 μM; Fig. 1A), which was designed as a structural negative control, as it cannot bind cellular iron and is not redox active [33,36,38]; and (2) DFO (250 μM; Fig. 1A), which is a "gold standard" iron chelator that does not induce redox stress [36,37]. Notably, DFO was used at 250 μM due to its low membrane permeability, as this agent is relatively hydrophilic [33,36,45].

As demonstrated previously [46], endogenous NDRG1 in control PANC1-VC cells was detected by immunoblotting as two main bands at ~41 and ~46 kDa (Fig. 1B). These two bands are consistent with multiple NDRG1 isoforms, which may be the result of truncation and/or phosphorylation [46,47]. Incubation of PANC1-VC cells with the negative control, Dp2mT, led to no significant ($p > 0.05$) effect relative to the control, while incubation PANC1-VC cells with either DFO or Dp44mT resulted in a significant ($p < 0.05$) increase in total NDRG1 expression *versus* the control (Fig. 1B). This was the result of an increase in the ~46 kDa NDRG1 band and an additional far more intense ~47 kDa NDRG1 band also being detected. These data were similar to those reported for other cell-types after incubation with DFO and Dp44mT [46].

Examining PANC1-N1 control cells, a pronounced and significant ($p < 0.05$) increase in a band at ~48 kDa was observed that is consistent with exogenous NDRG1 containing a FLAG tag (Fig. 1B). As such, under all treatment conditions in PANC1-N1 cells, NDRG1 was significantly ($p < 0.01$–0.05) increased relative to corresponding treatments in PANC1-VC cells. Incubation of PANC1-N1 cells with Dp2mT did not markedly alter NDRG1 levels relative to the respective control, while DFO and Dp44mT slightly, but not significantly ($p > 0.05$), increased NDRG1 levels *versus* the PANC1-N1 control (Fig. 1B). Notably, NDRG1 expression is also examined as a relevant control in all later studies (*i.e.*, Figs. 3B, 4–6) that utilize the same experimental setup as that in Fig. 1B, with consistent results being observed throughout.

Collectively, these studies demonstrate that both DFO and Dp44mT substantially increase the expression of NDRG1 in PANC1-VC cells, with these agents also slightly increasing NDRG1 in PANC1-N1 cells.

3.2. Only NDRG1 expression increases calnexin levels, while both NDRG1 and Dp44mT increase expression of the ER chaperones, calreticulin and BiP

The ER performs its protein-folding function with the help of three highly regulated ER chaperone proteins, namely: (1) calnexin; (2) calreticulin; and (3) BiP [1,7]. Previous investigations have suggested that calnexin may possess a potential NDRG1-binding site [48] and could have a role in tumor invasion and metastasis [49]. Moreover, calreticulin and BiP up-regulation has been documented in a multiple cancer-types [18,50–52]. Consequently, studies were initiated to assess the effect of NDRG1 and Dp44mT on the expression of the ER-associated chaperones, calnexin, calreticulin and BiP. In these experiments, PANC1-VC or PANC1-N1 NDRG1 over-expressing cells were incubated for 24 h/37 °C with control medium or this medium containing Dp2mT (10 μM), DFO (250 μM), or Dp44mT (10 μM) (Fig. 1C–E).

There was no significant ($p > 0.05$) change in calnexin levels following incubation with either Dp2mT, DFO, or Dp44mT compared to the control in PANC1-VC or PANC1-N1 cells (Fig. 1C). However, there was a significant ($p < 0.01$–0.05) increase in the expression of calnexin in PANC1-N1 cells relative to PANC1-VC cells under all incubation conditions (Fig. 1C).

Examining calreticulin expression, incubation with the negative control, Dp2mT, resulted in no significant ($p > 0.05$) change in calreticulin expression in PANC1-VC cells *versus* the control (Fig. 1D). However, calreticulin expression was significantly ($p < 0.01$) increased by DFO or Dp44mT treatment in PANC1-VC cells compared to the control (Fig. 1D). Interestingly, PANC1-N1 cells expressed significantly ($p < 0.001$) increased calreticulin levels in control or Dp2mT treatment conditions relative to the respective PANC1-VC controls (Fig. 1D). Similarly to PANC1-VC cells, incubation of PANC1-N1 cells with the negative control, Dp2mT, did not significantly ($p > 0.05$) alter the expression of calreticulin relative to the PANC1-N1 control. However, PANC1-N1 cells expressed slightly, but significantly ($p < 0.05$) increased calreticulin levels in the presence of DFO or Dp44mT relative to the PANC1-N1 control (Fig. 1D).

Assessment of BiP expression upon incubation of PANC1-VC cells with Dp2mT or DFO demonstrated no significant ($p > 0.05$) effect on its levels relative to the corresponding control (Fig. 1E). In contrast, Dp44mT significantly ($p < 0.001$) increased BiP expression relative to the respective PANC1-VC control. PANC1-N1 cells expressed significantly ($p < 0.001$–0.01) increased BiP levels under all conditions relative to the respective PANC1-VC cell treatments (Fig. 1E). Similarly to PANC1-VC cells, there was no significant ($p > 0.05$) change in BiP levels upon incubation with Dp2mT or DFO compared to the corresponding control in PANC1-N1 cells (Fig. 1E). However, BiP expression was significantly ($p < 0.001$) increased upon incubation with Dp44mT in PANC1-N1 cells compared to the relevant PANC1-N1 control.

Collectively, these studies in Fig. 1 demonstrate that NDRG1 over-expression significantly increases calnexin, calreticulin and BiP levels, with Dp44mT increasing the expression of calreticulin and BiP in the presence or absence of NDRG1 expression.

3.3. Confocal microscopy demonstrates that Dp44mT induces calreticulin co-localization with NDRG1, with NDRG1 over-expression alone increasing co-localization between NDRG1 and BiP

Considering the investigations assessing ER chaperone expression in Fig. 1, further studies using confocal immunofluorescence microscopy were performed. This was done to determine whether NDRG1 and/or Dp44mT altered their cellular localization, and if there was co-localization between NDRG1 and the chaperones to suggest potential binding (Fig. 2). In fact, NDRG1 has been shown to bind to other proteins to affect their half-life and expression [53] and confocal microscopy allows assessment on a single plane to enable conclusions on association to be made. Studies were performed in PANC1-VC and PANC1-N1 cells in the presence and absence of Dp44mT (10 μM) over a 24 h/37 °C incubation (Fig. 2). The Mander's coefficient (r) was generated using ImageJ and any value > 0.8 was considered indicative of strong molecular co-localization [54].

The distribution of calnexin in PANC1-VC control cells was predominantly cytoplasmic (Fig. 2A_1). NDRG1 demonstrated cytoplasmic staining with some nuclear distribution (Fig. 2A_2) when compared to the nuclear DAPI stain (Fig. 2A_3). The overlay demonstrated no substantial co-localization of NDRG1 and calnexin (Fig. 2$A_{4,5}$; $r = 0.794$). Following Dp44mT treatment, the intensity and distribution of calnexin in PANC1-VC cells did not significantly ($p > 0.05$) change (Fig. 2A_6). In contrast, after incubation of PANC1-VC cells with Dp44mT, NDRG1 intensity (Fig. 2A_7) increased significantly ($p < 0.01$) relative to the corresponding control (Fig. 2A_2) with no increase in the co-localization of calnexin and NDRG1 (Fig. 2$A_{9,10}$; $r = 0.558$).

The intensity of calnexin expression in the presence and absence of Dp44mT was significantly ($p < 0.01$) increased in PANC1-N1 cells (Fig. 2$A_{11,16}$) when compared to the respective PANC1-VC treatments (Fig. 2$A_{1,6}$). PANC1-N1 cells had significantly ($p < 0.001$–0.05) higher NDRG1 levels (Fig. 2$A_{12,17}$) in the presence and absence of Dp44mT, when compared to the respective PANC1-VC cells (Fig. 2$A_{2,7}$). The overlay demonstrated no marked or significant increase in the co-localization intensity of calnexin and NDRG1 in PANC1-N1 cells in the presence of the control (Fig. 2$A_{13,15}$) or Dp44mT (Fig. 2$A_{19,20}$), as demonstrated by $r = 0.784$ or 0.687, respectively.

Examining control PANC1-VC cells, calreticulin (Fig. 2B_1) and NDRG1 (Fig. 2B_2) were distributed in both the cytoplasm and nucleus, with $r = 0.720$ in terms of the overlay (Fig. 2$B_{4,5}$). As evident from the western analysis (Fig. 1D), calreticulin (Fig. 2B_6) and NDRG1 (Fig. 2B_7) intensity was significantly ($p < 0.001$) increased in PANC1-VC cells after incubation with Dp44mT relative to their respective controls (Fig. 2$B_{1,2}$). Furthermore, Dp44mT significantly ($p < 0.001$) increased the co-localization intensity of calreticulin and NDRG1 in PANC1-VC cells (Fig. 2$B_{9,10}$), resulting in $r = 0.860$.

The intensity of calreticulin (Fig. 2B_{11}) and NDRG1 (Fig. 2B_{12}) expression was significantly ($p < 0.001$) increased in PANC1-N1 control cells relative to their PANC1-VC counterparts (Fig. 2$B_{1,2}$). Again, Dp44mT significantly ($p < 0.01$) increased calreticulin intensity in PANC1-N1 cells (Fig. 2B_{16}) relative to the PANC1-N1 control cells (Fig. 2B_{11}), as also demonstrated by immunoblotting (Fig. 1D). The significantly ($p < 0.01$) increased co-localization intensity of calreticulin and NDRG1 in Dp44mT-treated PANC1-N1 cells (Fig. 2$B_{19,20}$; $r = 0.804$) relative to the respective PANC1-N1 control.

Similarly to calreticulin, both BiP (Fig. 2C_1) and NDRG1 (Fig. 2C_2) were distributed in the cytoplasm and nucleus in PANC1-VC cells with $r = 0.651$. Following Dp44mT treatment, BiP (Fig. 2C_6) and NDRG1 (Fig. 2C_7) intensity and co-localization (Fig. 2$C_{9,10}$) was significantly ($p < 0.05$) increased in PANC1-VC cells relative to the respective controls (Fig. 2$C_{1,2}$), confirming the western blot results (Fig. 1E).

Moreover, the intensity of BiP (Fig. 2C_{11}) and NDRG1 (Fig. 2C_{12}) expression was significantly higher ($p < 0.001$–0.01) in PANC1-N1 control cells relative to the respective PANC1-VC controls (Fig. 2$C_{1,2}$). The co-localization intensity of BiP and NDRG1 (Fig. 2$C_{14,15}$) in PANC1-N1 control cells was significantly ($p < 0.01$) increased relative to the PANC1-VC control (Fig. 2$C_{4,5}$), resulting in $r = 0.930$. Incubation of PANC1-N1 cells with Dp44mT significantly ($p < 0.001$) increased the intensity of BiP (Fig. 2C_{16}) relative to the respective PANC1-N1 control (Fig. 2C_{11}). There was also a significant ($p < 0.05$) increase in the co-localization intensity between BiP and NDRG1 in Dp44mT-treated PANC1-N1 cells (Fig. 2$C_{19,20}$) relative to the respective Dp44mT-treated PANC1-VC cells (Fig. 2$C_{9,10}$), leading to an increase in r from 0.798 to 0.925.

In summary, Dp44mT increases calreticulin co-localization with NDRG1 in the presence and absence of NDRG1 over-expression, with NDRG1 over-expression alone increasing co-localization between NDRG1 and BiP. On the other hand, neither Dp44mT nor NDRG1 over-expression alone or together, had any significant effect on co-localization of calnexin and NDRG1.

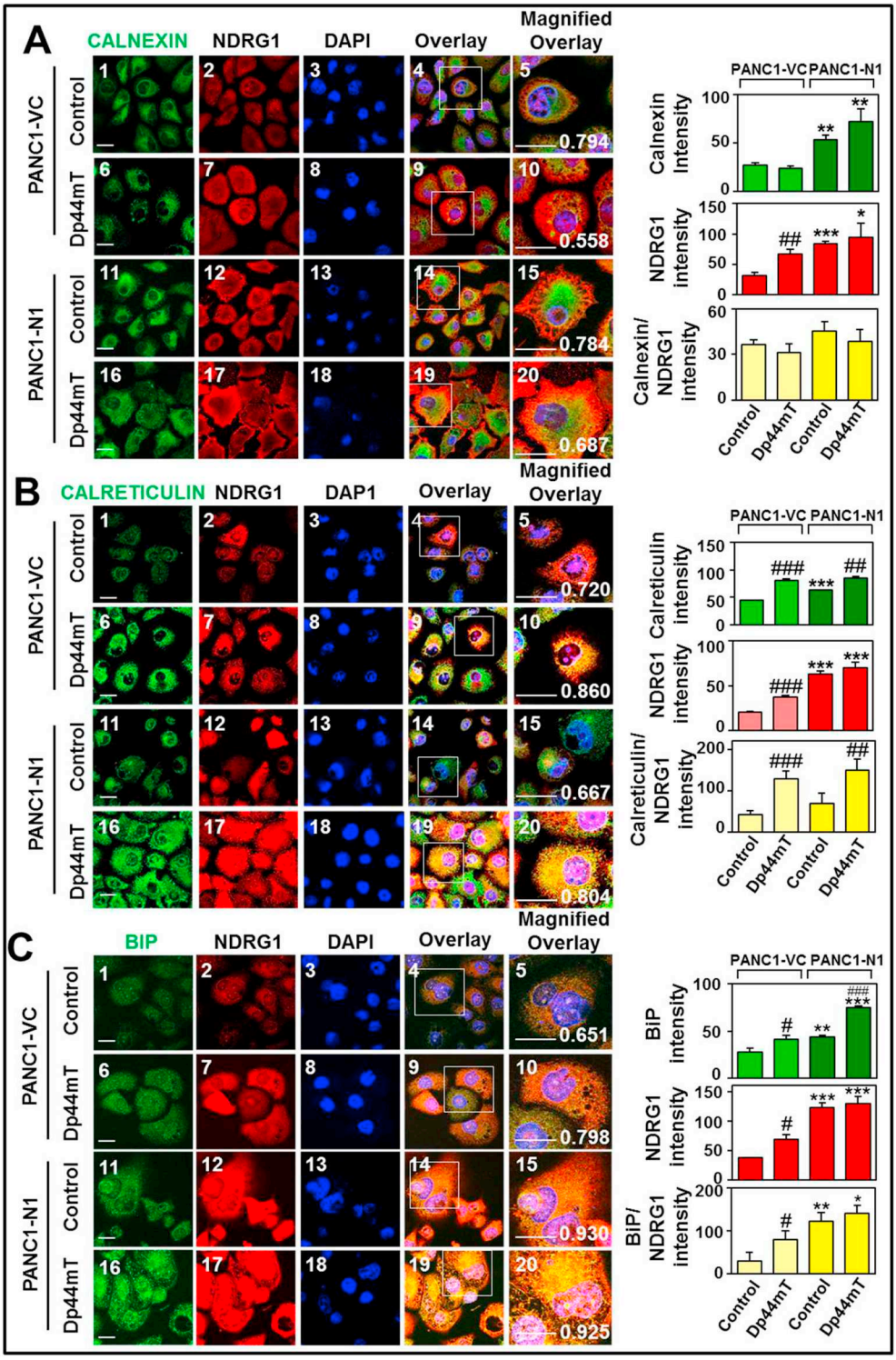

Fig. 2. Dp44mT induces co-localization of calreticulin with NDRG1, while NDRG1 over-expression alone increases co-localization of NDRG1 and BiP. PANC1-VC and PANC1-N1 cells were incubated for 24 h/37 °C with control media or media containing Dp44mT (10 μM). All cells were then probed for NDRG1 (red) and nuclei (blue). Cells were also probed for: (A) calnexin (green), (B) calreticulin (green), or (C) BiP (green). Images were taken using a Zeiss LSM Meta Spectral Confocal Microscope at 63× magnification using the same exposure time for all images. Mander's coefficient (*r*) and comparative fluorescence intensity (A.U.) were generated using ImageJ and is a representative of three experiments. Fluorescence intensity is presented as a mean ± SEM of the intensity of each cell in the image. The *scale bar* in the *bottom left-hand corner* of the first image represents 20 μm and is the same across all images, including the *scale bar* in the *magnified overlay panel*. $^{\#}p < 0.05$, $^{\#\#}p < 0.01$, $^{\#\#\#}p < 0.001$; relative to respective controls $^{*}p < 0.05$, $^{**}p < 0.01$, $^{***}p < 0.001$; relative to their corresponding treatments in PANC1-VC cells.

3.4. Dp44mT-mediated NDRG1 expression moderates Ca^{+2} homeostasis in the ER

Calreticulin binds Ca^{+2}, with > 50% of Ca^{+2} in the ER associating with this protein [55]. Notably, NDRG1 is also referred to as calcium-associated protein 43 (Cap43), because it is regulated and activated in response to Ca^{+2} [56]. Consequently, in order to dissect the relationship between ER stress, NDRG1 and intracellular Ca^{+2} levels, studies examining cytosolic Ca^{+2} levels were undertaken using PANC1-VC and PANC1-N1 cells following treatment for 24 h/37 °C with either: control media, Dp2mT (10 μM), DFO (250 μM), or Dp44mT (10 μM; Fig. 3A). Our studies examined the fluorescence of the membrane-permeable, Ca^{+2}-binding probe, Fura-2 AM, in PANC1-VC and PANC1-N1 cells, as this probe detects Ca^{+2} in the cytosol [34,57].

After a 24 h/37 °C incubation, Dp2mT or DFO did not significantly ($p > 0.05$) alter Ca^{+2} levels relative to the control in PANC1-VC cells (Fig. 3A). In contrast, Dp44mT significantly ($p < 0.001$) increased cytosolic Ca^{+2} levels in PANC1-VC cells compared to the respective control cells (Fig. 3A). No significant ($p > 0.05$) change in Ca^{+2} levels were observed comparing PANC1-VC and PANC1-N1 control cells,

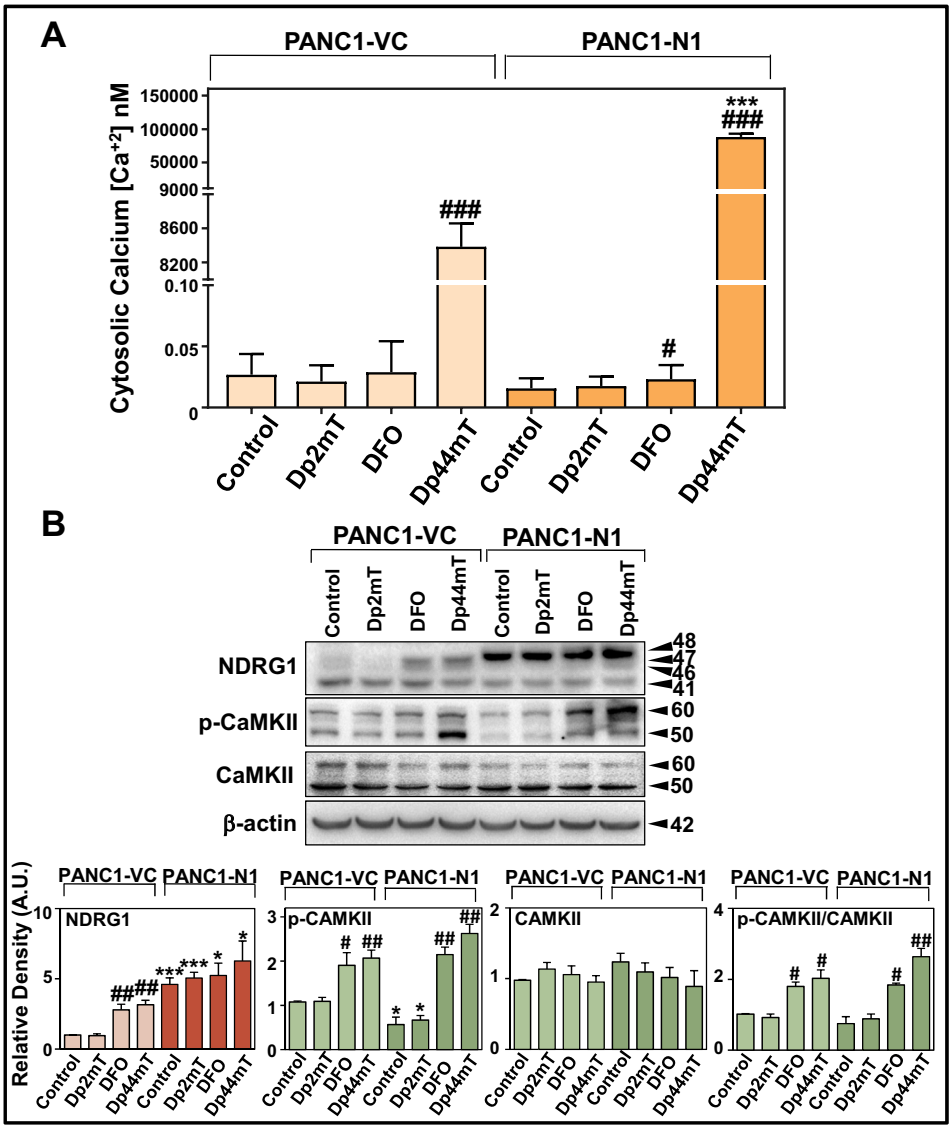

Fig. 3. Dp44mT-mediated treatment increases cytosolic Ca^{+2} levels in PANC1-VC and particularly PANC1-N1 cells and activates the Ca^{+2}/calmodulin-dependent kinase (CAMKII) cascade. PANC1-VC and PANC1-N1 cells were incubated for 24 h/37 °C with either control media, or media containing Dp2mT (10 μM), DFO (250 μM), or Dp44mT (10 μM). (A) PANC1-VC and PANC1-N1 cells were then incubated with Fura-2 AM dye for 30 min/37 °C to measure cytosolic calcium (Ca^{2+}) levels. Dp44mT induces an increase in cytosolic Ca^{+2} in both PANC1-VC and PANC1-N1 cells. (B) p-CAMKII expression is increased in response to Dp44mT and decreased in NDRG1 over-expressing control cells. Expression of CAMKII is unchanged in response to Dp44mT or NDRG1. (A–B) Results are typical of at least three experiments and is represented as mean ± SEM (3 experiments). (B) The densitometric analysis is normalized to β-actin (A.U.). $^{\#}p < 0.05$, $^{\#\#}p < 0.01$, $^{\#\#\#}p < 0.001$: treatment relative to respective control, $^{*}p < 0.05$, $^{**}p < 0.01$, $^{***}p < 0.001$; relative to corresponding treatments in PANC1-VC cells.

suggesting that NDRG1 does not modulate cytosolic Ca^{+2} levels. Similarly to PANC1-VC cells, Dp2mT did not significantly ($p > 0.05$) change Ca^{+2} levels in comparison to the PANC1-N1 control cells. Conversely, DFO and, to a markedly greater extent, Dp44mT, significantly ($p < 0.001$–0.05) increased the concentration of cytosolic Ca^{+2} in PANC1-N1 cells (Fig. 3A). In fact, the cytosolic Ca^{+2} levels of Dp44mT-treated PANC1-N1 cells were significantly ($p < 0.001$) greater by almost 10-times than Dp44mT-treated PANC1-VC cells. These studies demonstrate NDRG1 expression causes pronounced sensitization of PANC1-N1 cells to the Dp44mT-induced release of Ca^{+2} into the cytosol.

Elevated Ca^{+2} release from the ER results in an increase of the cytosolic Ca^{+2} concentration ($[Ca^{+2}]_C$), which is known to activate a Ca^{+2}/calmodulin-dependent kinase (CaMK) cascade resulting in the phosphorylation and activation of CaMKII [58]. Since Dp44mT markedly and significantly ($p < 0.001$) increased cytosolic Ca^{+2} concentrations (Fig. 3A), we investigated whether it increased activated and phosphorylated CaMKII levels (Fig. 3B). As evident in Fig. 3B, and consistent with previous studies [59], p-CaMKII and CaMKII were detected at two distinct bands at ~50 kDa and ~60 kDa, that are representative of its α and β subunits.

The negative control for Dp44mT, namely Dp2mT [33], did not significantly ($p > 0.05$) alter p-CaMKII levels relative to the control in PANC1-VC cells (Fig. 3B). Conversely, DFO and particularly Dp44mT, resulted in a significant ($p < 0.05$–0.01) increase in p-CaMKII levels in PANC1-VC cells (Fig. 3B). Of note, p-CaMKII levels were significantly ($p < 0.05$) reduced in control and Dp2mT-treated PANC1-N1 cells relative to their corresponding PANC1-VC counterparts. Similarly to PANC1-VC cells, DFO and Dp44mT significantly ($p < 0.01$) increased p-CaMKII levels in PANC1-N1 cells relative to the PANC1-N1 control. There was no significant ($p > 0.05$) change in total CaMKII under all treatment conditions examined in PANC1-VC or PANC1-N1 cells (Fig. 3B). In terms of the p-CaMKII/CaMKII ratio, Dp2mT did not significantly ($p > 0.05$) alter the ratio of p-CaMKII/CaMKII in PANC1-VC or PANC1-N1 cells (Fig. 3B). In contrast, incubation of PANC1-VC and PANC1-N1 cells with DFO or Dp44mT significantly ($p < 0.01$–0.05) increased the ratio of p-CaMKII/CaMKII compared to the respective PANC1-VC and PANC1-N1 controls (Fig. 3B).

Collectively, these results demonstrate that Dp44mT increased the activation of CaMKII in both PANC1-VC and PANC1-N1 cells, with NDRG1 expression not significantly affecting this process. Hence, the levels of cytosolic Ca^{+2} particularly in PANC1-N1 cells treated with Dp44mT did not directly correlate to the activation of CAMKII, suggesting that NDRG1 expression more markedly affected Ca^{+2} mobilization under these conditions.

3.5. NDRG1 suppresses the PERK signaling pathway and potentiates the downstream effects of Dp44mT

Considering the alterations to ER resident chaperone proteins and intracellular Ca^{+2} levels after NDRG1 expression and/or incubation of cells with the strong NDRG1-inducer Dp44mT, studies progressed to assess the relationship between NDRG1 and the three main pathways of the UPR, namely: (1) PERK; (2) IRE1α; and (3) ATF6 pathways. Initially, the PERK axis and its downstream targets were assessed [60]. Activated p-PERK phosphorylates eIF2α, leading to inhibition of cap-dependent protein translation, and paradoxically, also induces ATF4 up-regulation, which leads to the transcription of the pro-apoptotic gene, *CHOP* [60].

The PERK axis and its downstream targets, namely, p-eIF2α, ATF4 and CHOP, were investigated after a 24 h/37 °C incubation with control medium, or this medium containing Dp2mT (10 μM), DFO (250 μM), or Dp44mT (10 μM). Relative to the respective controls, there was no significant ($p > 0.05$) effect on p-PERK levels upon incubation with Dp2mT in PANC1-VC or PANC1-N1 cells (Fig. 4). PANC1-VC cells treated with DFO showed significantly ($p < 0.05$) decreased expression of p-PERK when compared with PANC1-VC control cells. In contrast, PANC1-VC cells incubated with Dp44mT demonstrated a pronounced and significant ($p < 0.01$) increase in p-PERK levels compared to their respective control (Fig. 4). Over-expression of NDRG1 in PANC1-N1 cells resulted in significantly ($p < 0.05$) decreased p-PERK levels in control or Dp2mT-treated cells relative to the respective treatments in PANC1-VC cells. Further, NDRG1 over-expression in PANC1-N1 cells resulted in a marked and significant ($p < 0.05$) suppression of Dp44mT-induced up-regulation of p-PERK levels *versus* the respective PANC1-VC treatment (Fig. 4). Similar effects of Dp44mT and NDRG1 over-expression on p-PERK levels were also demonstrated in HT-29 colon cancer cells transfected with NDRG1 (HT29-N1) relative to the VC (HT29-VC; Supplementary Fig. 1).

In terms of total PERK levels, Dp2mT or DFO had no significant ($p > 0.05$) effect, while Dp44mT induced a slight, but significant ($p < 0.05$) increase in total PERK compared to the control in PANC1-VC cells (Fig. 4). NDRG1 over-expression in PANC1-N1 cells resulted in a significant ($p < 0.001$–0.05) decrease in total PERK expression compared to PANC1-VC cells under all conditions (Fig. 4). Dp44mT significantly ($p < 0.01$) increased the ratio of p-PERK/PERK expression in PANC1-VC cells, while this effect was significantly ($p < 0.01$) attenuated by NDRG1 expression in PANC1-N1 cells. Again, broadly similar effects of Dp44mT and NDRG1 over-expression on total PERK levels and the p-PERK/PERK ratio were also demonstrated in HT29 colon cancer cells (*i.e.*, HT29-N1 *versus* HT29-VC; Supplementary Fig. 1).

Activation of the PERK axis results in the phosphorylation of eIF2α and consequent up-regulation of ATF4, which leads to transcription of *CHOP* [61]. The negative control, Dp2mT, did not exhibit any significant ($p > 0.05$) effect on p-eIF2α levels in PANC1-VC and PANC1-N1 cells relative to their respective controls (Fig. 4). In contrast, in both PANC1-VC and PANC1-N1 cells, there was a significant ($p < 0.001$–0.01) increase in p-eIF2α levels following incubation with DFO or Dp44mT compared to their respective controls (Fig. 4). Interestingly, NDRG1 over-expression in PANC1-N1 cells resulted in a significant ($p < 0.01$) decrease in p-eIF2α levels in cells incubated with control medium or Dp2mT relative to the correspondingly treated PANC1-VC cells (Fig. 4). However, NDRG1 expression in PANC1-N1 cells, significantly ($p < 0.01$–0.05) increased p-eIF2α levels in cells incubated with DFO and Dp44mT relative to their PANC1-VC counterparts. Total eIF2α levels were not significantly ($p > 0.05$) affected relative to the respective controls under all conditions.

Both DFO and Dp44mT significantly ($p < 0.01$) increased the ratio of p-eIF2α/eIF2α in PANC1-VC cells relative to the respective control, with this effect being significantly ($p < 0.001$–0.05) enhanced by these agents in PANC1-N1 cells (Fig. 4). In conjunction with the results observed for PERK, these data demonstrate that Dp44mT induces ER stress *via* the PERK-eIF2α axis, with NDRG1 suppressing PERK phosphorylation. These data reveal that while DFO does not induce PERK phosphorylation, eIF2α was activated by DFO in both PANC1-VC and PANC1–N1 cells (Fig. 4). Collectively, these results indicate differences in response between the activation of PERK and its downstream target, eIF2α, suggesting that additional regulatory mechanisms may activate eIF2α. Considering this, other upstream kinases such as protein kinase activated by double-stranded RNA (PKR [62]), heme-regulated

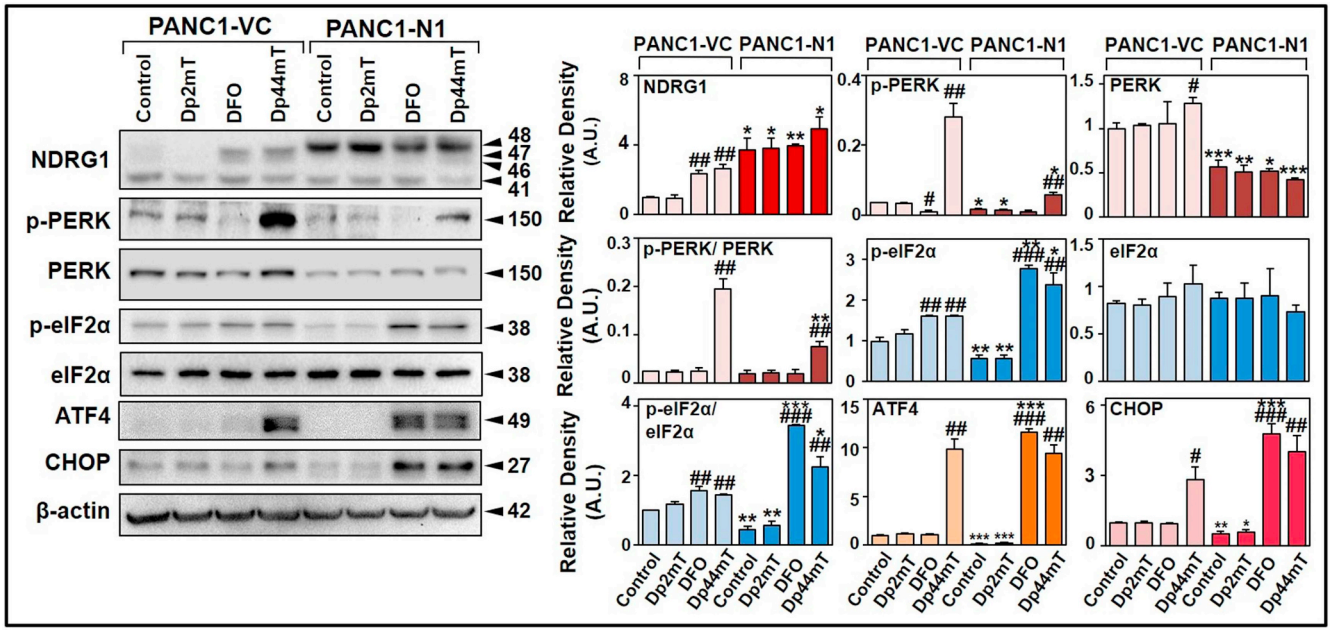

Fig. 4. The effect of NDRG1 expression and Dp2mT, DFO and Dp44mT on the PERK signaling pathway. PANC1-VC and PANC1-N1 cells were incubated with either control media, or media containing Dp2mT (10 μM), DFO (250 μM) or Dp44mT (10 μM) at 37 °C/24 h. Expression of p-PERK, PERK, p-eIF2α, eIF2α, ATF4 and CHOP was then determined. Western blot represents a typical blot and densitometric analysis is presented as mean ± SEM (3 experiments) normalized to β-actin (A.U.). $^{\#}p < 0.05$, $^{\#\#}p < 0.01$, $^{\#\#\#}p < 0.001$; relative to respective controls $^{*}p < 0.05$, $^{**}p < 0.01$, $^{***}p < 0.001$; relative to corresponding treatments in PANC1-VC cells.

inhibitor activated by heme-deficiency (HRI [63]) and general control non-derepressible-2 (GCN2 [64]), are also known to phosphorylate eIF2α.

After a 24 h incubation of PANC1-VC cells with Dp2mT or DFO, ATF4 expression did not change significantly ($p > 0.05$) relative to the control, while there was a pronounced and significant ($p < 0.01$) increase after incubation with Dp44mT (Fig. 4). In PANC1-N1 cells, ATF4 expression was significantly ($p < 0.001$) decreased after incubation with control medium or Dp2mT relative to the respective PANC1-VC cells (Fig. 4). There was a significant ($p < 0.001$–0.01) increase in ATF4 in PANC1-N1 cells incubated with DFO or Dp44mT relative to the respective PANC1-N1 control (Fig. 4). Similar results to those found for ATF4 were also observed with the expression of the downstream pro-apoptotic protein, CHOP. The ability of DFO to induce an increase in p-eIF2α levels, but not ATF4 or CHOP expression, in PANC1-VC cells, may be a time-dependent effect and further time points could be useful to elucidate this.

In summary, the results in Fig. 4 demonstrated that NDRG1 over-expression resulted in the basal suppression of PERK phosphorylation, but on the other hand, generally potentiated the ER-stress-inducing effects of DFO and Dp44mT on p-eIF2α, ATF4 and CHOP levels.

3.6. NDRG1 expression suppresses the pro-apoptotic pathways of the IRE1α axis, while increasing its pro-survival signals

The effect of the agents and NDRG1 expression on the IRE1α signaling cascade was subsequently examined (Fig. 5). IRE1α catalyzes the unconventional processing of *XBP1* splicing, which in turn, regulates UPR target genes, such as BiP and p58^{IPK} [65]. In addition to the XBP1-dependent pathway, IRE1α activates an additional pathway through c-Jun NH_2-terminal kinase (JNK), which mediates apoptosis [5]. Therefore, the expression of total IRE1α, the active phosphorylated IRE1α (p-IRE1α) and its downstream regulatory molecules, unspliced XBP1 (XBP1u), spliced XBP1s (XBP1s), p58^{IPK}, p-JNK and total JNK, were examined to assess regulation (Fig. 5).

Following incubation with Dp2mT or DFO, there was no significant alteration in the levels of p-IRE1α relative to the control in PANC1-VC cells (Fig. 5). In contrast, there was a significant ($p < 0.05$) increase in p-IRE1α levels in Dp44mT-treated PANC1-VC cells compared to the PANC1-VC control. Interestingly, in PANC1-N1 cells incubated with control medium or Dp2mT, NDRG1 over-expression resulted in a significant ($p < 0.001$–0.01) decrease in p-IRE1α levels relative to the respective PANC1-VC cell treatments (Fig. 5). On the other hand, DFO slightly increased p-IRE1α levels relative to the PANC1-N1 control, while Dp44mT induced a significant ($p < 0.01$) increase in p-IRE1α levels compared to the PANC1-N1 control (Fig. 5).

Examining total IRE1α levels, a similar effect was observed as found for p-IRE1α in response to the agents (Fig. 5). Again, Dp44mT significantly ($p < 0.001$) increased total IRE1α expression in PANC1-VC cells relative to the respective control. For PANC1-N1 cells, a significant ($p < 0.01$–0.05) decrease in total IRE1α was observed for the control and Dp2mT relative to the respective PANC1-VC cells (Fig. 5). On the other hand, PANC1-N1 cells displayed a significant ($p < 0.01$) increase in total-IRE1α levels with both DFO and Dp44mT relative to the respective PANC1-N1 control (Fig. 5). Assessing the ratio of p-IRE1α/total IRE1α in PANC1-VC cells, Dp44mT slightly, but significantly ($p < 0.01$), reduced the ratio relative to the respective control. In PANC1-N1 cells, the p-IRE1α/total IRE1α ratio was significantly ($p < 0.05$) reduced in control- and Dp2mT-treated PANC1-N1 cells relative to the respective treatments in PANC1-VC cells (Fig. 5). Similar effects of NDRG1 over-expression suppressing the activity of Dp44mT on up-regulating p-IRE1α and IRE1α levels were also observed in HT29 colon cancer cells (Supplementary Fig. 1).

Next, examining XBP1s expression in PANC1-VC cells, Dp2mT and DFO had no significant effect relative to the respective control, while Dp44mT had a significant ($p < 0.01$) inhibitory effect on XBP1s levels relative to the respective PANC1-VC control (Fig. 5). A significant ($p < 0.01$–0.05) increase in XBP1s levels was observed in control and Dp2mT-treated PANC1-N1 cells relative to the PANC1-VC control

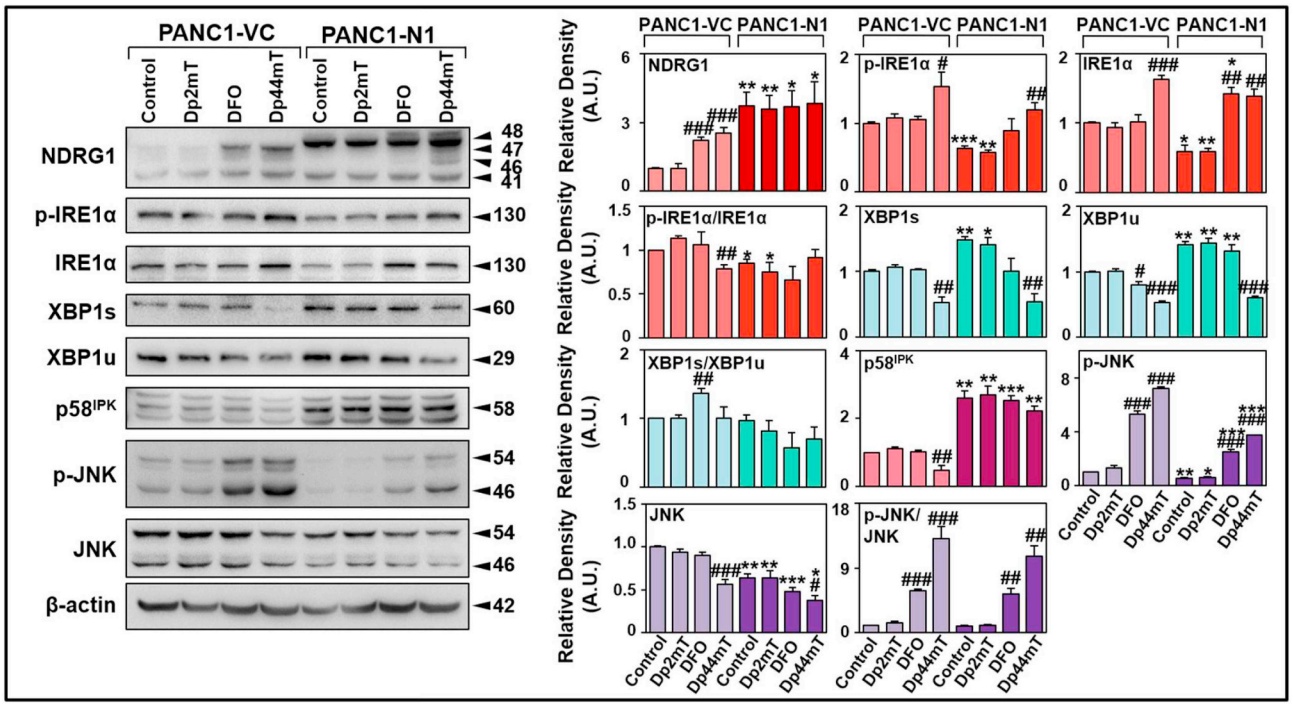

Fig. 5. The effect of NDRG1 expression and Dp2mT, DFO and Dp44mT on the IRE1α signaling pathway. PANC1-VC and PANC1-N1 cells were incubated with either control media, or media containing: Dp2mT (10 μM), DFO (250 μM) or Dp44mT (10 μM) at 24 h/37 °C. Following this the expression of p-IRE1α, IRE1α, XBP1s, XBP1u, p58^{IPK}, p-JNK and JNK was determined. Western blot represents a typical blot and densitometric analysis is presented as mean ± SEM (3 experiments) normalized to β-actin (A.U.). $^{\#}p < 0.05$, $^{\#\#}p < 0.01$, $^{\#\#\#}p < 0.001$; relative to respective controls $^{*}p < 0.05$, $^{**}p < 0.01$, $^{***}p < 0.001$; relative to corresponding treatments in PANC1-VC cells.

(Fig. 5). While DFO slightly decreased XBP1s levels relative to control PANC1-N1 cells, only Dp44mT was effective at significantly ($p < 0.01$) decreasing XBP1s expression relative to the PANC1-N1 control. Similar results to those found for XBP1s were also observed for XBP1u after the treatments (Fig. 5). Analyzing the XBP1s/XBP1u ratio, only DFO significantly ($p < 0.01$) increased the XBP1s/XBP1u ratio in PANC1-VC cells relative to its respective control, which was due to the lack of change in XBP1s and decrease in XBP1u levels (Fig. 5).

Three distinct bands for $p58^{IPK}$ between ~50–60 kDa were observed, with a band at ~58 kDa being the most prominent (Fig. 5). It has been reported that $p58^{IPK}$ contains a cleavable ER signal sequence [66], suggesting the multiple bands may be cleaved isoforms. The densitometry herein analyzed the most prominent band at ~58 kDa. Examining PANC1-VC cells, $p58^{IPK}$ levels were significantly ($p < 0.01$) decreased by Dp44mT relative to the respective control. The expression of $p58^{IPK}$ was significantly ($p < 0.001$–0.01) increased under all incubation conditions in PANC1-N1 cells compared to the respective PANC1-VC cell treatments (Fig. 5). Furthermore, Dp2mT, DFO, or Dp44mT, had no significant effect on $p58^{IPK}$ levels relative to the respective control in PANC1-N1 cells (Fig. 5). The generalized increase of $p58^{IPK}$ expression by NDRG1 over-expression may act to facilitate cellular survival.

As described previously, the kinase activity of IRE1α regulates an XBP1-independent pathway *via* TRAF2-ASK1-JNK signaling [5]. This latter mechanism plays a vital role in apoptotic signaling [32]. Consequently, total-JNK and p-JNK levels were examined to investigate the role of NDRG1 expression and the effect of chelators on this signaling pathway. Herein, the densitometric analysis of both total-JNK and p-JNK is the sum of the major bands observed at 46- and 54-kDa (Fig. 5), which represent different spliced isoforms [67,68]. Incubation of PANC1-VC and PANC1-N1 cells with DFO or Dp44mT markedly and significantly ($p < 0.001$) increased p-JNK levels relative to their corresponding controls (Fig. 5). However, NDRG1 over-expression resulted in a significant ($p < 0.001$–0.05) decrease in p-JNK levels in PANC1-N1 cells compared to their respective PANC1-VC clones under all conditions.

Total-JNK expression was significantly ($p < 0.001$–0.05) suppressed in PANC1-VC and PANC1-N1 cells by only Dp44mT compared to the respective controls. Over-expression of NDRG1 in PANC1-N1 cells demonstrated a significant ($p < 0.001$–0.05) decrease in total-JNK expression compared to their respective PANC1-VC treatments under all incubation conditions (Fig. 5). Both DFO and Dp44mT markedly and significantly ($p < 0.001$–0.01) increased the ratio of p-JNK/total JNK levels similarly in PANC1-VC and PANC1-N1 cells relative to their respective controls.

Overall, these results in Fig. 5 demonstrated that NDRG1 suppressed the pro-apoptotic arms of the IRE1α pathway (*i.e.*, p-JNK), while increasing the pro-survival signaling pathways (*i.e.*, XBP1s and $p58^{IPK}$). Conversely, the anti-cancer agent, Dp44mT, inhibited the pro-survival pathways (*i.e.*, XBP1s) and induced phosphorylation of the pro-apoptotic p-JNK pathway.

3.7. NDRG1 and Dp44mT promote ATF6 cleavage

The ATF6 survival pathway is activated once BiP dissociates from ATF6 in the ER, enabling its subsequent cleavage and activation [69]. Considering this, western analysis was performed to compare the levels of cleaved ATF6 in PANC1-VC and PANC1-N1 cells, following incubation with either control medium, Dp2mT (10 μM), DFO (250 μM), or Dp44mT (10 μM) for 24 h/37 °C (Fig. 6). It has been reported that cleaved ATF6 is observed as two distinct bands at ~36 kDa and ~75 kDa [69–72], which was confirmed herein (Fig. 6).

Following a 24 h/37 °C incubation, Dp2mT or DFO did not significantly ($p > 0.05$) alter the expression of the cleaved 75-kDa form of ATF6 in PANC1-VC cells, while Dp44mT significantly ($p < 0.05$) increased it relative to the respective control (Fig. 6). Notably, cleaved 75-kDa ATF6 expression was significantly ($p < 0.01$–0.05) increased in PANC1-N1 cells respective to PANC1-VC cells under all incubation conditions (Fig. 6). Examining expression of the 36-kDa cleaved form of ATF6 in PANC1-VC cells, only Dp44mT significantly ($p < 0.01$) increased its expression relative to the respective control (Fig. 6). Levels of the 36-kDa cleaved form of ATF6 was significantly ($p < 0.01$) higher in PANC1-N1 control or Dp2mT-treated cells compared to their respective PANC1-VC counterparts. In contrast, no significant difference was noted for DFO or Dp44mT in PANC1-N1 cells under these conditions, relative to their respective treatments in PANC1-VC cells (Fig. 6).

Overall, these results in Fig. 6 indicate NDRG1 over-expression and/or Dp44mT increase the 75-kDa cleaved ATF6 form. A similar although less pronounced effect was noted for the 36-kDa form, where Dp44mT increased ATF6 in PANC1-VC cells. Similar effects of NDRG1 and Dp44mT on ATF6 expression were also evident in HT29 colon cancer cells (Supplementary Fig. 1).

3.8. Silencing NDRG1 induces the phosphorylation of PERK and IRE1α and cleavage of ATF6

Additional studies assessed the effect of silencing NDRG1 *via* transient transfection with siRNA to examine the differential effect of NDRG1 expression on the three main UPR pathways in PANC1-VC cells relative to a negative control siRNA (NC siRNA; Fig. 7). In these experiments, Dp44mT was compared relative to the control, since of the agents examined, it induced the most marked effects in Figs. 1–6.

As reported previously [43,46], silencing NDRG1 (PANC1-VC siNDRG1) in both the control and Dp44mT-treated cells led to a marked and significant ($p < 0.01$) reduction in the 46- and 47-kDa NDRG1 bands, but not the 41-kDa band, relative to the NC siRNA-treated cells (Fig. 7). Down-regulating the upper NDRG1 band by siRNA is vital to prevent its downstream anti-oncogenic functions [53].

As observed using PANC1-VC and PANC1-N1 cells (Fig. 4), Dp44mT significantly ($p < 0.01$–0.05) increased p-PERK in both PANC1-VC NC siRNA and especially siNDRG1-treated cells relative to the corresponding controls (Fig. 7). In contrast to NDRG1 over-expression, which decreased p-PERK (Fig. 4), silencing NDRG1 significantly ($p < 0.001$) increased p-PERK levels in control cells relative to the respective NC siRNA (Fig. 7). A similar, yet less pronounced effect, was also observed with total PERK levels, which were significantly ($p < 0.01$) greater in control PANC1-VC siNDRG1 cells relative to control PANC1-VC NC siRNA cells (Fig. 7). The p-PERK/PERK ratio was significantly ($p < 0.01$–0.05) enhanced in Dp44mT-treated cells in both the NC siRNA and siNDRG1-treated cells *versus* their respective controls.

Incubation of PANC1-VC NC siRNA cells with Dp44mT significantly ($p < 0.01$–0.05) increased both p-IRE1α and total IRE1α relative to the respective controls (Fig. 7), as observed for PANC1-VC cells (Fig. 5). Silencing NDRG1 induced a significant ($p < 0.01$) increase in p-IRE1α and total IRE1α in control PANC1-VC siNDRG1 cells relative to control PANC1-VC NC siRNA cells (Fig. 7), while NDRG1 over-expression in the controls had the opposite effect (Fig. 5). Of note, NDRG1 over-expression in PANC1-N1 cells slightly suppressed p-IRE1α and total IRE1α levels after treatment with Dp44mT relative to the respective PANC1-VC Dp44mT-treated cells (Fig. 5). This was contrary to the effect of siNDRG1 in Dp44mT-treated PANC1-VC cells that slightly ($p > 0.05$) increased p-IRE1α and total IRE1α levels relative to PANC1-VC NC siRNA cells incubated with Dp44mT (Fig. 7). The ratio of p-IRE1α/IRE1α was not significantly altered under any treatment condition.

Silencing NDRG1 in control PANC1-VC cells resulted in a significant ($p < 0.01$) increase in cleaved ATF6 expression (36- and 75-kDa) relative to control NC siRNA cells (Fig. 7). This effect on cleaved ATF6 under control conditions was similar to the response obtained after NDRG1 hyper-expression in PANC1-N1 cells relative to PANC1-VC (Fig. 6). The reason for this similar response of cleaved ATF6 expression to NDRG1 siRNA and NDRG1 hyper-expression is unknown. In Dp44mT-treated cells, no significant change in cleaved ATF6 (36- and

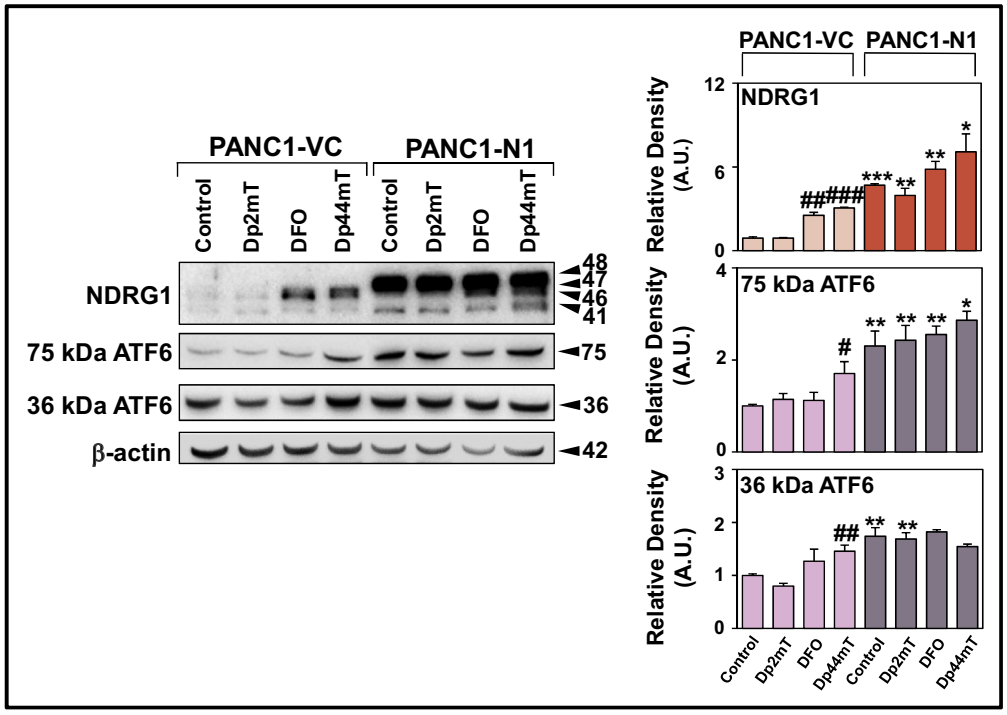

Fig. 6. Dp44mT and NDRG1 increase the expression of cleaved ATF6 (36 and 75 kDa). PANC1-VC and PANC1-N1 cells were incubated for 24 h/37 °C with control media or media containing: Dp2mT (10 μM), DFO (250 μM) or Dp44mT (10 μM). Results are representative of at least 3 experiments and densitometric analysis is presented as mean ± SEM (3 experiments) normalized to β-actin (A.U.). $^{\#}p < 0.05$, $^{\#\#}p < 0.01$, $^{\#\#\#}p < 0.001$; relative to respective controls $^{*}p < 0.05$, $^{**}p < 0.01$, $^{***}p < 0.001$; relative to corresponding treatments in PANC1-VC cells.

75-kDa) levels were observed upon silencing NDRG1 comparing PANC1-VC siNDRG1 to Dp44mT-treated PANC1-VC NC siRNA cells (Fig. 7).

Overall, these studies in Fig. 7, demonstrate that conversely to NDRG1 over-expression (Figs. 4–6), silencing NDRG1 generally resulted in an opposite effect, inducing activation of the PERK and IRE1α axis. In contrast, silencing and over-expression of NDRG1 had similar effects on cleaved ATF6.

3.9. Silencing PERK increases sensitivity to Dp44mT anti-proliferative activity, with NDRG1 expression enhancing Dp44mT efficacy in the presence or absence of PERK

Considering the potent effects of Dp44mT and NDRG1 on the UPR shown above (Figs. 1–7), the effect of silencing key molecules in each of the 3 arms, namely PERK, IRE1α and ATF6, in the presence and absence of NDRG1, was examined in terms of key oncogenic processes, namely

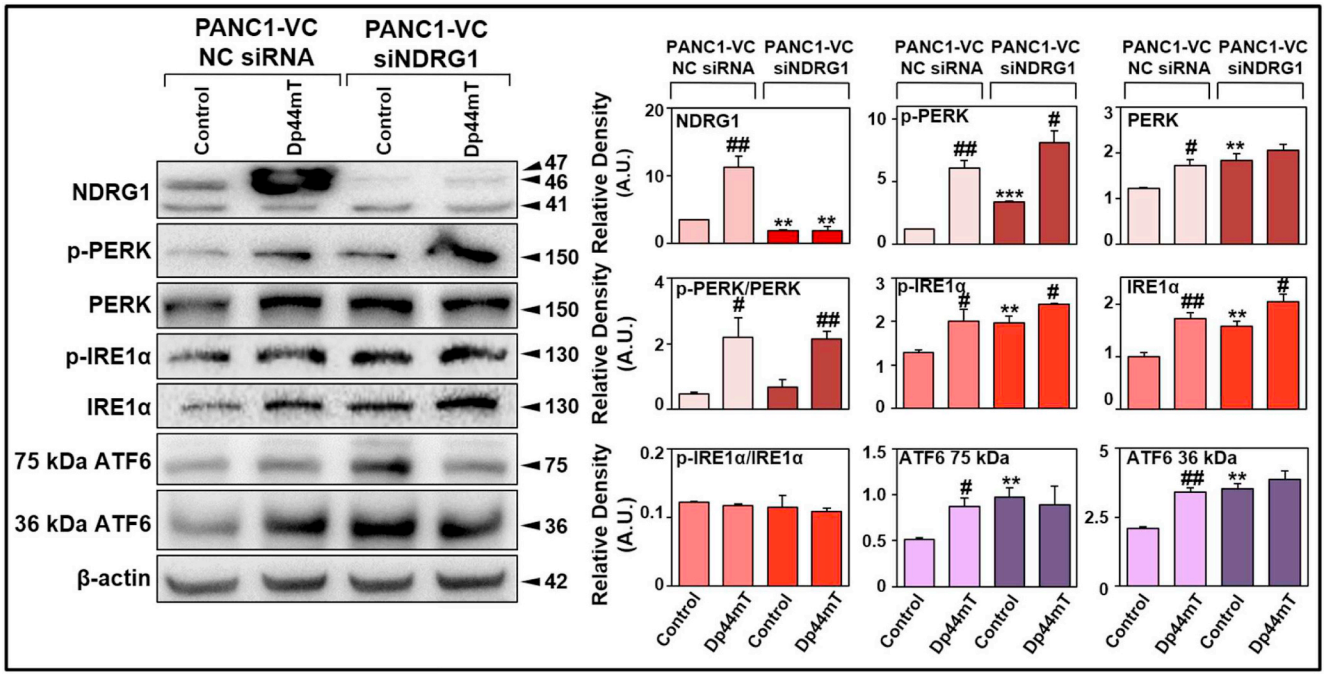

Fig. 7. The effect of NDRG1 silencing and Dp44mT on the activation of the ER stress pathways. PANC1 cells were incubated with control siRNA or siNDRG1, which was the followed by a 24 h/37 °C incubation with control media or media containing Dp44mT (10 μM). Western analysis was performed to determine the expression of NDRG1, p-PERK, PERK, p-IRE1α, IRE1α and cleaved ATF6. Results are representative of at least 3 experiments and densitometric analysis is presented as mean ± SEM (3 experiments) normalized to β-actin (A.U.). $^{\#}p < 0.05$, $^{\#\#}p < 0.01$, $^{\#\#\#}p < 0.001$ relative to respective controls. $^{*}p < 0.05$, $^{**}p < 0.01$, $^{***}p < 0.001$; relative to corresponding treatments in PANC1-VC cells.

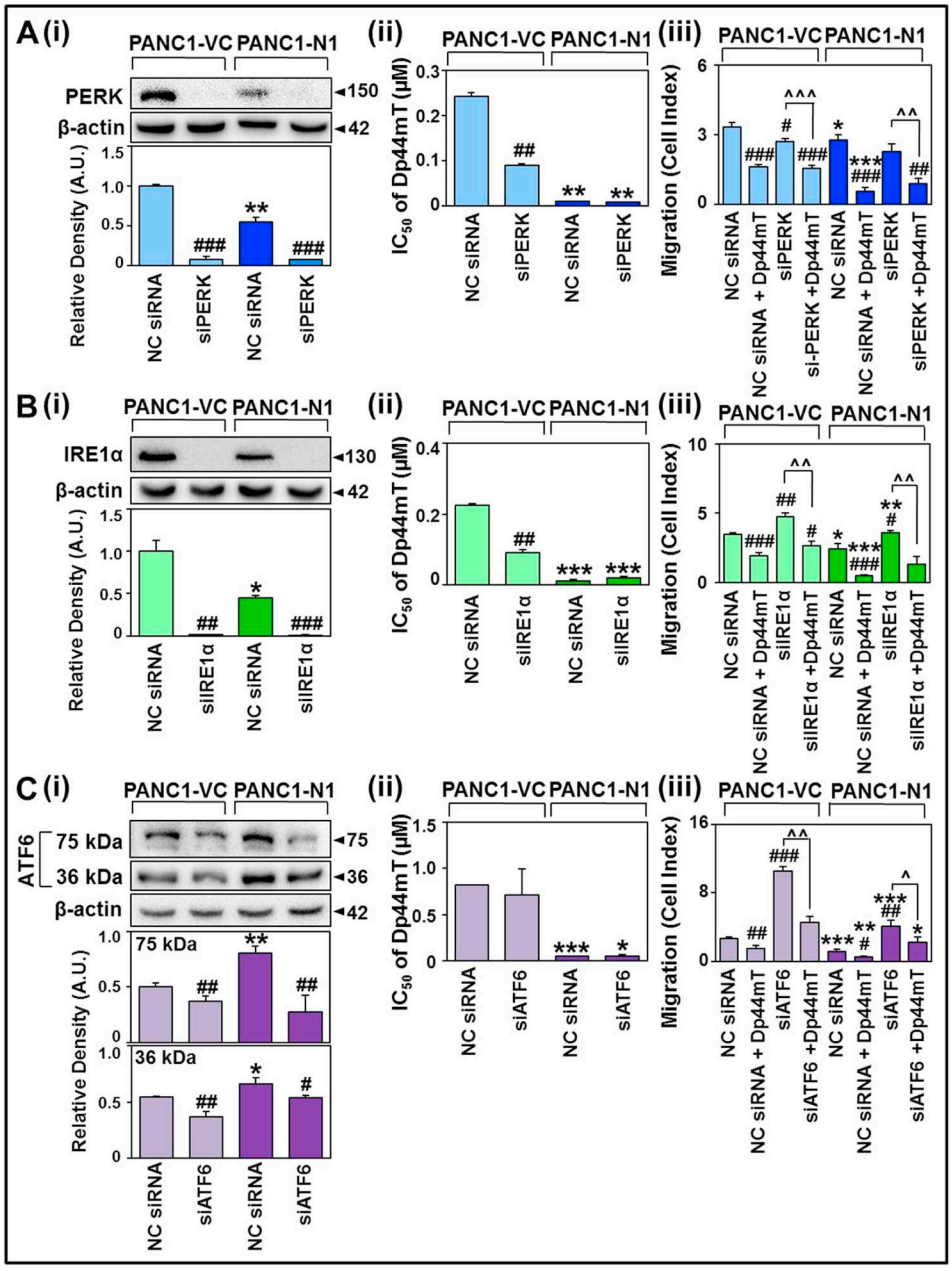

Fig. 8. Effect of silencing PERK, IRE1α, or ATF6 on proliferation and migration. PANC1-VC and PANC1-N1 cells were incubated with control siRNA or (A) siPERK, (B) siIRE1α, or (C) siATF6. (Ai–Ci) Western blotting was performed to examine silencing and are representative of a typical blot. Densitometric analysis is represented as mean ± SEM (3 experiments) normalized to β-actin (A.U.). (Aii, Bii, Cii) Cells were incubated with Dp44mT (0–10 μM) for 48 h/37 °C and the MTT proliferation assay was used to determine the IC_{50} values. The IC_{50} values are represented as mean ± SEM of 3 independent experiments, with at least two replicates per experiment. $^{\#}p < 0.05$, $^{\#\#}p < 0.01$, $^{\#\#\#}p < 0.001$; relative to respective controls. $^{*}p < 0.05$, $^{**}p < 0.01$, $^{***}p < 0.001$; relative to corresponding treatments in PANC1-VC cells. (Aiii, Biii, Ciii) Cells were incubated with control siRNA or siRNA for target protein and then incubated with control media or media containing Dp44mT (10 μM) for 24 h/37 °C. Cells were then plated on the 16-well Xcelligence real-time assay plate in the absence of Dp44mT. Migration over 48 h/37 °C was recorded as cell index (A.U.). Each independent experiment (n = 3–4) has a minimum of two replicates/experiment. $^{\#}p < 0.05$, $^{\#\#}p < 0.01$, $^{\#\#\#}p < 0.001$; relative to respective controls. $^{*}p < 0.05$, $^{**}p < 0.01$, $^{***}p < 0.001$; relative to the corresponding treatments in PANC1-VC cells. $^{\wedge}p < 0.05$, $^{\wedge\wedge}p < 0.01$, $^{\wedge\wedge\wedge}p < 0.001$; relative to the corresponding treatments outlined in the graph.

proliferation and migration (Fig. 8A–C).

PERK siRNA relative to its NC siRNA was utilized in the presence or absence of Dp44mT to determine its effect on proliferation over an incubation of 48 h/37 °C (Fig. 8A). Transfection with *PERK* siRNA (si-PERK) significantly ($p < 0.001$) decreased PERK expression in PANC1-VC and PANC1-N1 cells relative to the respective NC siRNA-treated cells (Fig. 8Ai). As shown in Fig. 4, again NDRG1 over-expression in the PANC1-N1 control cells (*i.e.*, NC siRNA) significantly ($p < 0.01$) decreased total PERK levels relative to PANC1-VC NC siRNA (Fig. 8Ai).

Next, the anti-proliferative activity of Dp44mT in PANC1-VC and PANC1-N1 cells was examined through IC_{50} value measurements over 48 h/37 °C (Fig. 8Aii). A significant ($p < 0.01$) reduction in the IC_{50} was evident in siPERK-treated PANC1-VC cells relative to the PANC1-VC NC siRNA-treated cells (Fig. 8Aii). Additionally, the IC_{50} of Dp44mT was markedly and significantly ($p < 0.01$) reduced in PANC1-N1 cells transfected with either NC siRNA or siPERK relative to the respective treatments in PANC1-VC cells.

In summary, Dp44mT is effective at inhibiting proliferation under all conditions (Fig. 8Aii). However, PERK expression is protective against Dp44mT anti-proliferative activity in PANC1-VC cells, with NDRG1 over-expression ablating this protective effect. NDRG1 over-expression in PANC1-N1 cells leads to markedly greater sensitivity to Dp44mT anti-proliferative activity in either the presence or absence of PERK silencing.

3.10. Silencing PERK decreases migration, while NDRG1 over-expression enhances Dp44mT efficacy at inhibiting migration in the presence or absence of PERK

All studies examining migration (Fig. 8Aiii, Biii, Ciii) were performed with cells incubated with and without Dp44mT (10 μM) for 24 h/37 °C. The agent was then removed, cellular viability was assessed and found to be > 90%, and the effect on migration then evaluated over 48 h/37 °C. This short incubation protocol was specifically implemented to minimise the cytotoxic effect of Dp44mT on migration (see Materials and methods). These studies revealed that Dp44mT

significantly ($p < 0.001$) decreased migration of PANC1-VC cells relative to the NC siRNA control in either the presence of NC siRNA or siPERK (Fig. 8Aiii). siPERK alone also slightly, but significantly ($p < 0.05$), reduced migration of PANC1-VC cells relative to the respective NC siRNA. Notably, PANC1-VC cells incubated with a combination of siPERK and Dp44mT showed a significant ($p < 0.001$) reduction in migration relative to cells incubation with PERK siRNA alone (Fig. 8Aiii).

The control (*i.e.*, NC siRNA) NDRG1 over-expressing (PANC1-N1) cells migrated slightly, but significantly ($p < 0.05$) less than control PANC1-VC cells (Fig. 8Aiii). As evident in PANC1-VC cells, PANC1-N1 cells incubated with Dp44mT and NC siRNA or siPERK migrated significantly ($p < 0.001$–0.01) less than control PANC1-N1 NC siRNA cells. The effect of Dp44mT at inhibiting migration was more effective in the presence of NDRG1 over-expression with or without siPERK treatment *versus* the respective PANC1-VC treatments. Collectively, NDRG1 expression alone decreased migration and Dp44mT inhibited migration under all conditions, irrespective of PERK expression, and decreasing PERK expression alone inhibited migration.

3.11. Silencing IRE1α increases sensitivity to Dp44mT anti-proliferative activity, with NDRG1 expression markedly enhancing Dp44mT efficacy in the presence or absence of IRE1α

IRE1α siRNA relative to its NC siRNA (Fig. 8Bi) was utilized in the presence or absence of Dp44mT to determine its effect on proliferation over 48 h/37 °C (Fig. 8Bii). *IRE1α* siRNA markedly and significantly ($p < 0.001$–0.01) decreased IRE1α expression in both PANC1-VC and PANC1–N1 cells relative to the NC siRNA (Fig. 8Bi). Additionally, as shown in Fig. 5, NDRG1 expression in NC siRNA PANC1-N1 cells significantly ($p < 0.05$) decreased IRE1α levels relative to NC siRNA PANC1-VC cells (Fig. 8Bi).

Similarly to the *PERK* siRNA studies (Fig. 8Aii), a significant ($p < 0.01$) reduction in the IC_{50} of Dp44mT was evident in siIRE1α-treated PANC1-VC cells relative to NC siRNA-treated PANC1-VC cells (Fig. 8Bii). Moreover, the IC_{50} of Dp44mT was markedly ($p < 0.001$) reduced in PANC1-N1 cells transfected with NC siRNA or siIRE1α relative to the respective PANC1-VC cells (Fig. 8Bii). Combined, these results demonstrate that IRE1α expression protects against Dp44mT-induced cytotoxicity, while NDRG1 over-expression potently increases Dp44mT anti-proliferative efficacy in the presence or absence of IRE1α.

3.12. Silencing IRE1α increases migration, with NDRG1 expression and/or Dp44mT decreasing migration in the presence of IRE1α, but not after siIREα treatment

The treatment of PANC1-VC or PANC1-N1 cells with Dp44mT in addition to either NC siRNA or siIRE1α resulted in a significant ($p < 0.001$–0.01) decrease in migration relative to the respective siRNAs alone (Fig. 8Biii). Incubation of PANC1-N1 cells with NC siRNA significantly ($p < 0.05$) decreased migration relative to the NC siRNA in PANC1-VC cells. The addition of Dp44mT and siIRE1α to PANC1-N1 cells resulted in a slight, but not significant decrease in migration relative to NC siRNA in these cells. In both PANC1-VC and PANC1-N1 cells, siIRE1α alone increased ($p < 0.01$–0.05) migration relative to the respective NC siRNAs (Fig. 8Biii). In summary, IREα silencing increases migration, in contrast to NDRG1 and/or Dp44mT that inhibit cell migration.

3.13. Silencing ATF6 does not significantly alter the sensitivity to Dp44mT anti-proliferative activity, with NDRG1 expression enhancing Dp44mT anti-proliferative efficacy in the presence or absence of ATF6

Next, *ATF6* siRNA relative to its NC siRNA (Fig. 8Ci) was utilized in the presence or absence of Dp44mT to determine its effect on proliferation over 48 h/37 °C (Fig. 8Cii). ATF6 siRNA (siATF6) significantly ($p < 0.01$–0.05) reduced ATF6 levels (36- and 75-kDa bands) in PANC1-VC and PANC1-N1 cells (Fig. 8Ci). As shown in Fig. 6 for both the 36- and 75-kDa ATF6 bands, NDRG1 expression in PANC1-N1 significantly ($p < 0.01$–0.05) increased their levels under control conditions (*i.e.*, NC siRNA) relative to the PANC1-VC control (Fig. 8Ci).

Proliferation assays revealed that siATF6 did not significantly impact on the anti-proliferative activity (*i.e.*, IC_{50}) of Dp44mT in PANC1-VC cells, while the IC_{50} of Dp44mT was markedly ($p < 0.001$–0.05) reduced in PANC1-N1 cells transfected with either NC siRNA or siATF6 relative to the respective PANC1-VC cells (Fig. 8Cii). Thus, ATF6 expression does not affect Dp44mT anti-proliferative efficacy in PANC1-VC cells, while NDRG1 expression potently increases Dp44mT activity in the presence or absence of ATF6.

3.14. Silencing ATF6 markedly increases migration in PANC1-VC cells, which is inhibited by NDRG1 expression in the presence and absence of Dp44mT

Silencing ATF6 in both PANC1-VC and PANC1-N1 cells (Fig. 8Ci) markedly and significantly ($p < 0.001$–0.01) increased migration relative to the respective control NC siRNA (Fig. 8Ciii). The addition of Dp44mT in the presence of the control NC siRNA in both PANC1-VC and PANC1-N1 cells significantly ($p < 0.01$–0.05) decreased migration relative to their respective NC siRNA controls. A significant ($p < 0.01$–0.05) decrease in migration occurred in siATF6-treated PANC1-VC and PANC1-N1 cells incubated with Dp44mT relative to siATF6 alone (Fig. 8Ciii). NDRG1 expression in the NC siRNA, NC siRNA + Dp44mT, siATF6, and siATF6 + Dp44mT treatment conditions significantly ($p < 0.001$–0.05) decreased migration relative to their respective PANC1-VC cell conditions. Collectively, ATF6 silencing increased migration in PANC1-VC and PANC1-N1 cells, while NDRG1 suppressed migration under all conditions.

4. Discussion

The stress response protein, NDRG1, plays a critical role in regulating various cellular signaling pathways, including metastasis, proliferation, cell differentiation, angiogenesis, lipid synthesis and immunity [29,73,74]. Additionally, NDRG1 plays a role in the ER stress response, with NDRG1 suppressing the autophagic pathway through the PERK-eIF2α axis of the UPR [40]. Consequently, herein, the mechanisms underlying the ability of NDRG1 to mediate the ER stress response pathways were examined in-depth. The anti-cancer agent, Dp44mT, was also utilized throughout these studies, as it is well-known to up-regulate NDRG1 [75–77] and also induces ER stress through its pharmacological activity [34].

Our initial investigations focused on characterizing the effect of NDRG1 over-expression on the ER chaperones. These studies revealed that NDRG1 over-expression or Dp44mT treatment alone increased calreticulin and BiP expression. The most prominent effect on inducing the expression of these latter chaperones was observed when both NDRG1 expression and Dp44mT treatment were combined. In contrast, NDRG1, but not Dp44mT, increased calnexin expression. It can be hypothesized that NDRG1 or Dp44mT cause ER stress to activate the UPR, inducing the compensatory up-regulation of the key ER chaperones, calreticulin and BiP, to alleviate the stress response. The fact that NDRG1 expression alone caused increased calreticulin or BiP levels could be partially related to the mechanism of how Dp44mT also induces the expression of these chaperones, that is, *via* its well-known ability to up-regulate NDRG1 [30,31].

NDRG1 modulates the expression of proteins linked to vesicular transport, having a potential role in the vesicular recycling and

degradation pathway [53,78]. As such, the alterations in the expression of proteins in high NDRG1 expressing cells, such as BiP and calnexin, could be associated with ER membrane translocation. Considering this, a proteomics investigation has revealed that NDRG1 has a potential binding site with calnexin or BiP [48]. Interestingly, unlike calnexin, the current investigation demonstrated BiP co-localization with NDRG1 in NDRG1 over-expressing in the presence or absence of Dp44mT. These studies suggest that either NDRG1 is a target to be folded into correct conformation by chaperones and/or acts as a protein chaperone itself. The intriguing recent finding that NDRG1 binds directly to MIG6, which is a negative regulator of the epidermal growth factor receptor, also supports these observations [53,78].

The up-regulation of calreticulin by Dp44mT or NDRG1 alone, or synergistically by both, is of interest since: (1) a substantial quantity of Ca^{+2} in the ER binds to calreticulin [55]; and (2) NDRG1 is also referred to as calcium-associated protein 43 (Cap43), which is regulated and activated in response to Ca^{+2} [56]. An increase in cytosolic Ca^{+2} increases the sensitivity of cells to apoptosis *via* the CaMKII signaling cascade [79]. Of note, Dp44mT and particularly the combination of Dp44mT and NDRG1 expression were most effective in markedly increasing cytosolic Ca^{+2} levels. This could explain, at least in part, the potent anti-proliferative activity observed upon combining Dp44mT and NDRG1 over-expression. In good accordance with this observation, Dp44mT alone and particularly in combination with NDRG1, significantly increased p-CaMKII levels. As activation of CaMKII can subsequently activate pro-apoptotic JNK signaling, it was of some surprise to find the p-JNK was lower after NDRG1 over-expression. This could be related to the suppressive activity of NDRG1 expression on IRE1α signaling, which subsequently suppresses pro-apoptotic JNK activation [9]. Nonetheless, the pro-apoptotic activity of increased cytosolic Ca^{+2} [80] in the presence of both NDRG1 over-expression and Dp44mT could be at least one factor contributing to the potentiated cell death under these conditions relative to the control without NDRG1 over-expression.

In terms of the 3 classical arms of the UPR, the current studies indicate that NDRG1 expression alone suppressed the PERK-eIF2α-ATF4 pathway, decreasing pro-apoptotic CHOP expression. Further, the effect of Dp44mT in terms of potently inducing PERK phosphorylation and total PERK was markedly suppressed by NDRG1. However, a different response was observed for the downstream effectors of PERK signaling, whereby the presence of high NDRG1 expression in PANC1-N1 cells together with Dp44mT treatment resulted in: (1) markedly increased eIF2α activation; (2) the maintenance of ATF4 expression; and (3) an increase in pro-apoptotic CHOP expression relative to Dp44mT-treated PANC1-VC cells. These latter effects could again contribute to the greater cytotoxicity observed after incubation of cells over-expressing NDRG1 with Dp44mT. Silencing PERK in PANC1-VC cells led to increased Dp44mT cytotoxicity, suggesting that the effects of PERK signaling could be protective against the activity of this agent.

Regarding the second arm of the UPR mediated by IRE1α, NDRG1 suppressed IRE1α activation and its associated pro-apoptotic downstream target, JNK, while enhancing expression of its pro-survival signals, namely, XBP1s and $p58^{IPK}$. The incubation of NDRG1 over-expressing cells with Dp44mT increased the phosphorylation and activation of IRE1α relative to PANC1-N1 cells incubated with control medium. In contrast to XBP1s, incubation of PANC1-N1 cells with Dp44mT failed to decrease pro-survival $p58^{IPK}$, and while p-JNK was increased by Dp44mT, it remained significantly less than that observed after incubating PANC1-VC cells with Dp44mT. The pro-survival effects of the IRE1α pathway (*i.e.*, *via* XBP1 splicing and $p58^{IPK}$) may explain why silencing IRE1α in PANC1-VC cells leads to greater cytotoxicity relative to the NC siRNA. The fact that NDRG1 over-expression potentiates the cytotoxic effect of Dp44mT, may not relate to their effects on this pathway, but potentially to other effectors (*e.g.*, the PERK pathway).

We next investigated whether NDRG1 and Dp44mT influenced the third arm of the UPR, namely the ATF6 pathway. Our studies demonstrated that NDRG1 over-expression or Dp44mT significantly increased ATF6 cleavage. While ATF6 may initially trigger a pro-survival response, under chronic or severe stress, ATF6 may also promote pro-apoptotic pathways [1,4,81]. In fact, a downstream target of ATF6 is the pro-apoptotic protein, CHOP, which was shown to be inhibited by NDRG1 expression and increased by Dp44mT especially in the presence of NDRG1 over-expression. Again, the pronounced increase in anti-proliferative activity of Dp44mT in the presence of NDRG1 expression would agree with the marked up-regulation of pro-apoptotic CHOP under these conditions. Further, the fact that ATF6 silencing had little influence on Dp44mT-mediated cytotoxicity in PANC1-VC cells, indicates the requirement for NDRG1 over-expression for optimal effects of potentiating cell death induced by Dp44mT.

Apart from the marked effects of NDRG1 over-expression at inhibiting proliferation in the presence of Dp44mT, NDRG1 over-expression inhibited migration, which is in line with its ability to act as a metastasis suppressor [23,24]. Optimal anti-migratory activity was observed in the presence of both NDRG1 over-expression and Dp44mT treatment, which may relate to total NDRG1 levels which are highest under this condition. The silencing of PERK resulted in a decrease in migration, demonstrating its potential role in stimulated migration. Interestingly, the silencing of IRE1α or ATF6 in PANC1-VC cells increased migration relative to the respective controls, suggesting these molecules may inhibit metastasis. Nonetheless, this stimulation of migration, after both IRE1α or ATF6 silencing, was significantly decreased by Dp44mT in control and NDRG1 over-expressing cells. PERK has been implicated in migratory regulation of cells through the PERK-eIF2α-ATF4-LAMP3 pathway in various cancer-types [82,83]. In fact, UPR signaling is activated during the epithelial-mesenchymal transition (EMT), triggering PERK-eIF2α signaling [84]. Nevertheless, it is important to gain further information regarding which downstream UPR pathways are activated during the EMT to decipher whether its activation increases the pro-survival or pro-apoptotic pathways of the UPR.

5. Conclusion

NDRG1 is a multi-functional protein that interacts closely with multiple cellular pathways, including the ER and the UPR (Fig. 9). An important finding was that NDRG1 over-expression enhances the anti-proliferative and anti-migratory activity of Dp44mT, which could be related to the following effects in the presence of both Dp44mT and NDRG1, namely: (1) markedly increased eIF2α activation; (2) the maintenance of ATF4 expression; (3) the pronounced elevation in cytosolic Ca^{+2} that increases the sensitivity of cells to apoptosis *via* activation of CaMKII signaling cascade; and (4) increased pro-apoptotic CHOP expression. These studies provide further understanding into the pleiotropic functions of NDRG1 to further characterize its anti-oncogenic role in cancer and in the anti-tumor efficacy of the potent di-2-pyridylketone thiosemicarbazones.

Supplementary data to this article can be found online at https://doi.org/10.1016/j.bbadis.2019.04.007.

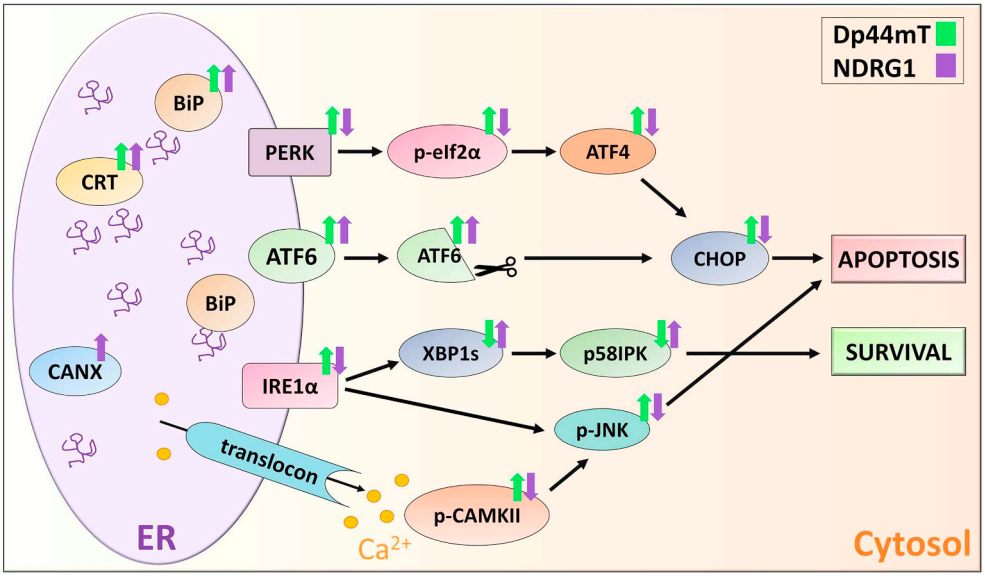

Fig. 9. Schematic diagram showing the effects of Dp44mT and NDRG1 on the UPR pathway. The cytotoxic iron chelator, Dp44mT, binds cellular metal ions and produces redox active iron complexes to generate ROS [33,35,37,38]. This agent affects the UPR pathway *via*: (1) the overt activation of PERK-eIF2α-ATF4 pathway that results in an increased pro-apoptotic CHOP expression; (2) a reduction in the expression of the pro-survival IRE1α pathway, namely, XBP1s and $p58^{IPK}$; (3) increased ATF6 cleavage that further potentiates pro-apoptotic CHOP expression; (4) enhanced expression of the ER resident proteins, BiP and calreticulin; and (5) increased Ca^{2+} signaling that activates CaMKII-JNK pro-apoptotic signaling. Interestingly, over-expression of the metastasis suppressor, NDRG1, on its own, elicits an opposite, pro-survival outcome from the alterations in UPR pathways. Most notably, NDRG1 reduces pro-apoptotic CHOP expression and enhances pro-survival XBP1s and $p58^{IPK}$ expression relative to Dp44mT. However, the combination of NDRG1 over-expression and Dp44mT treatment results in an enhancement of anti-cancer response, as indicated by the inhibition of proliferation and migration.

Transparency document

The Transparency document associated with this article can be found, in online version.

Acknowledgments

A.M.M. thanks the National Health and Medical Research Council for a Peter Doherty Fellowship (APP1105671), the Cancer Institute NSW for an Early Career Fellowship (15/ECF/1-08) and the University of New South Wales for a Scientia Fellowship. A.M.M. is also kindly supported by grant #1144868 awarded through the 2017 Priority-driven Collaborative Cancer Research Scheme and co-funded by Cancer Australia and Cure Cancer Australia Foundation, supported by the Can Too Foundation. The contents of the published material are solely the responsibility of the Administering Institutions, Participating Institutions or individual authors and do not reflect the views of NHMRC or Cancer Australia. S.S. appreciates a Young Investigator PdCCRS Grant jointly funded by Cancer Australia and the Cure Cancer Australia Foundation. S.S. also thanks AMP Foundation for the AMP Tomorrow Fund grant. D.R.R. appreciates a Senior Principal Research Fellowship and Project Grant funding from the National Health and Medical Research Council of Australia and a Priority-driven Collaborative Cancer Research Scheme (PdCCRS) Grant from Cancer Australia (Australian Government).

References

[1] C. Hetz, The unfolded protein response: controlling cell fate decisions under ER stress and beyond, Nat. Rev. Mol. Cell Biol. 13 (2012) 89–102.
[2] D.T. Rutkowski, R.J. Kaufman, A trip to the ER: coping with stress, Trends Cell Biol. 14 (2004) 20–28.
[3] D. Ron, P. Walter, Signal integration in the endoplasmic reticulum unfolded protein response, Nat. Rev. Mol. Cell Biol. 8 (2007) 519–529.
[4] C. Hetz, E. Chevet, S.A. Oakes, Proteostasis control by the unfolded protein response, Nat. Cell Biol. 17 (2015) 829–838.
[5] F. Urano, X. Wang, A. Bertolotti, Y. Zhang, P. Chung, H.P. Harding, D. Ron, Coupling of stress in the ER to activation of JNK protein kinases by transmembrane protein kinase IRE1, Science 287 (2000) 664–666.
[6] J.S. Shen, X. Chen, L. Hendershot, R. Prywes, ER stress regulation of ATF6 localization by dissociation of BiP/GRP78 binding and unmasking of golgi localization signals, Dev. Cell 3 (2002) 99–111.
[7] Y. Ma, L.M. Hendershot, The role of the unfolded protein response in tumour development: friend or foe? Nat. Rev. Cancer 4 (2004) 966–977.
[8] I. Kim, W. Xu, J.C. Reed, Cell death and endoplasmic reticulum stress: disease relevance and therapeutic opportunities, Nat. Rev. Drug Discov. 7 (2008) 1013–1030.
[9] Y.C. Tsai, A.M. Weissman, The unfolded protein response, degradation from endoplasmic reticulum and cancer, Genes Cancer 1 (2010) 764–778.
[10] M. Wang, R.J. Kaufman, The impact of the endoplasmic reticulum protein-folding environment on cancer development, Nat. Rev. Cancer 14 (2014) 581–597.
[11] H. Urra, E. Dufey, T. Avril, E. Chevet, C. Hetz, Endoplasmic reticulum stress and the hallmarks of cancer, Trends Cancer 2 (2016) 252–262.
[12] H.J. Clarke, J.E. Chambers, E. Liniker, S.J. Marciniak, Endoplasmic reticulum stress in malignancy, Cancer Cell 25 (2014) 563–573.
[13] S.S. Tan, I. Ahmad, H.L. Bennett, L. Singh, C. Nixon, M. Seywright, R.J. Barnetson, J. Edwards, H.Y. Leung, GRP78 up-regulation is associated with androgen receptor status, Hsp70-Hsp90 client proteins and castrate-resistant prostate cancer, J. Pathol. 223 (2011) 81–87.
[14] L. Pootrakul, R.H. Datar, S.R. Shi, J. Cai, D. Hawes, S.G. Groshen, A.S. Lee, R.J. Cote, Expression of stress response protein Grp78 is associated with the development of castration-resistant prostate cancer, Clin. Cancer Res. 12 (2006) 5987–5993.
[15] M. Shuda, N. Kondoh, N. Imazeki, K. Tanaka, T. Okada, K. Mori, A. Hada, M. Arai, T. Wakatsuki, O. Matsubara, N. Yamamoto, M. Yamamoto, Activation of the ATF6, XBP1 and grp78 genes in human hepatocellular carcinoma: a possible involvement of the ER stress pathway in hepatocarcinogenesis, J. Hepatol. 38 (2003) 605–614.
[16] X. Xing, M. Lai, Y. Wang, E. Xu, Q. Huang, Overexpression of glucose-regulated protein 78 in colon cancer, Clin. Chim. Acta 364 (2006) 308–315.
[17] J.A. Ehrenfried, B.E. Herron, C.M. Townsend, B.M. Evers, Heat-shock proteins are differentially expressed in human gastrointestinal cancers, Surg. Oncol. 4 (1995) 197–203.
[18] Z. Niu, M. Wang, L. Zhou, L. Yao, Q. Liao, Y. Zhao, Elevated GRP78 expression is associated with poor prognosis in patients with pancreatic cancer, Sci. Rep. 5 (2015) 16067.
[19] M. Hanaoka, T. Ishikawa, M. Ishiguro, M. Tokura, S. Yamauchi, A. Kikuchi, H. Uetake, M. Yasuno, T. Kawano, Expression of ATF6 as a marker of pre-cancerous atypical change in ulcerative colitis-associated colorectal cancer: a potential role in the management of dysplasia, J. Gastroenterol. 53 (2018) 631–641.
[20] J.M. Brown, A.J. Giaccia, The unique physiology of solid tumors: opportunities (and problems) for cancer therapy, Cancer Res. 58 (1998) 1408–1416.
[21] R.K. Yadav, S.W. Chae, H.R. Kim, H.J. Chae, Endoplasmic reticulum stress and cancer, J. Cancer Prev. 19 (2014) 75–88.
[22] M.A. Shah, N. Kemeny, A. Hummer, M. Drobnjak, M. Motwani, C. Cordon-Cardo, M. Gonen, G.K. Schwartz, Drg1 expression in 131 colorectal liver metastases: correlation with clinical variables and patient outcomes, Clin. Cancer Res. 11 (2005) 3296–3302.
[23] S. Bandyopadhyay, S.K. Pai, S.C. Gross, S. Hirota, S. Hosobe, K. Miura, K. Saito, T. Commes, S. Hayashi, M. Watabe, K. Watabe, The Drg-1 gene suppresses tumor metastasis in prostate cancer, Cancer Res. 63 (2003) 1731–1736.
[24] S. Bandyopadhyay, S.K. Pai, S. Hirota, S. Hosobe, Y. Takano, K. Saito, D. Piquemal, T. Commes, M. Watabe, S.C. Gross, Y. Wang, S. Ran, K. Watabe, Role of the putative tumor metastasis suppressor gene Drg-1 in breast cancer progression, Oncogene 23 (2004) 5675–5681.
[25] Y. Maruyama, M. Ono, A. Kawahara, T. Yokoyama, Y. Basaki, M. Kage, S. Aoyagi, H. Kinoshita, M. Kuwano, Tumor growth suppression in pancreatic cancer by a

putative metastasis suppressor gene Cap43/NDRG1/Drg-1 through modulation of angiogenesis, Cancer Res. 66 (2006) 6233–6242.
[26] J.R. Hickok, S. Sahni, Y. Mikhed, M.G. Bonini, D.D. Thomas, Nitric oxide suppresses tumor cell migration through N-Myc downstream-regulated gene-1 (NDRG1) expression: role of chelatable iron, J. Biol. Chem. 286 (2011) 41413–41424.
[27] R.J. Guan, H.L. Ford, Y. Fu, Y. Li, L.M. Shaw, A.B. Pardee, Drg-1 as a differentiation-related, putative metastatic suppressor gene in human colon cancer, Cancer Res. 60 (2000) 749–755.
[28] T.P. Ellen, Q. Ke, P. Zhang, M. Costa, NDRG1, a growth and cancer related gene: regulation of gene expression and function in normal and disease states, Carcinogenesis 29 (2008) 2–8.
[29] B.A. Fang, Z. Kovacevic, K.C. Park, D.S. Kalinowski, P.J. Jansson, D.J. Lane, S. Sahni, D.R. Richardson, Molecular functions of the iron-regulated metastasis suppressor, NDRG1, and its potential as a molecular target for cancer therapy, Biochim. Biophys. Acta 1845 (2014) 1–19.
[30] N.T. Le, D.R. Richardson, Iron chelators with high antiproliferative activity up-regulate the expression of a growth inhibitory and metastasis suppressor gene: a link between iron metabolism and proliferation, Blood 104 (2004) 2967–2975.
[31] D.J. Lane, F. Saletta, Y. Suryo Rahmanto, Z. Kovacevic, D.R. Richardson, N-myc downstream regulated 1 (NDRG1) is regulated by eukaryotic initiation factor 3a (eIF3a) during cellular stress caused by iron depletion, PLoS One 8 (2013) e57273.
[32] D.J. Lane, T.M. Mills, N.H. Shafie, A.M. Merlot, R. Saleh Moussa, D.S. Kalinowski, Z. Kovacevic, D.R. Richardson, Expanding horizons in iron chelation and the treatment of cancer: role of iron in the regulation of ER stress and the epithelial-mesenchymal transition, Biochim. Biophys. Acta 1845 (2014) 166–181.
[33] J. Yuan, D.B. Lovejoy, D.R. Richardson, Novel di-2-pyridyl-derived iron chelators with marked and selective antitumor activity: in vitro and in vivo assessment, Blood 104 (2004) 1450–1458.
[34] A.M. Merlot, N.H. Shafie, Y. Yu, V. Richardson, P.J. Jansson, S. Sahni, D.J.R. Lane, Z. Kovacevic, D.S. Kalinowski, D.R. Richardson, Mechanism of the induction of endoplasmic reticulum stress by the anti-cancer agent, di-2-pyridylketone 4,4-dimethyl-3-thiosemicarbazone (Dp44mT): activation of PERK/eIF2alpha, IRE1alpha, ATF6 and calmodulin kinase, Biochem. Pharmacol. 109 (2016) 27–47.
[35] D.B. Lovejoy, P.J. Jansson, U.T. Brunk, J. Wong, P. Ponka, D.R. Richardson, Antitumor activity of metal-chelating compound Dp44mT is mediated by formation of a redox-active copper complex that accumulates in lysosomes, Cancer Res. 71 (2011) 5871–5880.
[36] A.M. Merlot, D.S. Kalinowski, D.R. Richardson, Novel chelators for cancer treatment: where are we now? Antioxid. Redox Signal. 18 (2013) 973–1006.
[37] A.M. Merlot, D.S. Kalinowski, Z. Kovacevic, P.J. Jansson, S. Sahni, M.L. Huang, D.L. Lane, H. Lok, D.R. Richardson, Exploiting cancer metal metabolism using anticancer metal-binding agents, Curr. Med. Chem. 26 (2019) 302–322.
[38] D.R. Richardson, P.C. Sharpe, D.B. Lovejoy, D. Senaratne, D.S. Kalinowski, M. Islam, P.V. Bernhardt, Dipyridyl thiosemicarbazone chelators with potent and selective antitumor activity form iron complexes with redox activity, J. Med. Chem. 49 (2006) 6510–6521.
[39] A.M. Merlot, N. Pantarat, S.V. Menezes, S. Sahni, D.R. Richardson, D.S. Kalinowski, Cellular uptake of the antitumor agent Dp44mT occurs via a carrier/receptor-mediated mechanism, Mol. Pharmacol. 84 (2013) 911–924.
[40] S. Sahni, D.H. Bae, D.J. Lane, Z. Kovacevic, D.S. Kalinowski, P.J. Jansson, D.R. Richardson, The metastasis suppressor, N-myc downstream-regulated gene 1 (NDRG1), inhibits stress-induced autophagy in cancer cells, J. Biol. Chem. 289 (2014) 9692–9709.
[41] D.R. Richardson, E.H. Tran, P. Ponka, The potential of iron chelators of the pyridoxal isonicotinoyl hydrazone class as effective antiproliferative agents, Blood 86 (1995) 4295–4306.
[42] Z. Kovacevic, S. Chikhani, G.Y. Lui, S. Sivagurunathan, D.R. Richardson, The iron-regulated metastasis suppressor NDRG1 targets NEDD4L, PTEN, and SMAD4 and inhibits the PI3K and Ras signaling pathways, Antioxid. Redox Signal. 18 (2013) 874–887.
[43] Z. Chen, D. Zhang, F. Yue, M. Zheng, Z. Kovacevic, D.R. Richardson, The iron chelators Dp44mT and DFO inhibit TGF-beta-induced epithelial-mesenchymal transition via up-regulation of N-Myc downstream-regulated gene 1 (NDRG1), J. Biol. Chem. 287 (2012) 17016–17028.
[44] T. Arnould, C. Michiels, I. Alexandre, J. Remacle, Effect of hypoxia upon intracellular calcium concentration of human endothelial cells, J. Cell. Physiol. 152 (1992) 215–221.
[45] D. Richardson, P. Ponka, E. Baker, The effect of the iron(III) chelator, desferrioxamine, on iron and transferrin uptake by the human malignant melanoma cell, Cancer Res. 54 (1994) 685–689.
[46] K.C. Park, S.V. Menezes, D.S. Kalinowski, S. Sahni, P.J. Jansson, Z. Kovacevic, D.R. Richardson, Identification of differential phosphorylation and sub-cellular localization of the metastasis suppressor, Ndrg1, Biochim. Biophys. Acta 1864 (2018) 2644–2663.
[47] M.K. Ghalayini, Q. Dong, D.R. Richardson, S.J. Assinder, Proteolytic cleavage and truncation of NDRG1 in human prostate cancer cells, but not normal prostate epithelial cells, Biosci. Rep. 33 (2013).
[48] L.C. Tu, X. Yan, L. Hood, B. Lin, Proteomics analysis of the interactome of N-myc downstream regulated gene 1 and its interactions with the androgen response program in prostate cancer cells, Mol. Cell. Proteomics 6 (2007) 575–588.
[49] A. Okayama, Y. Miyagi, F. Oshita, M. Nishi, Y. Nakamura, Y. Nagashima, K. Akimoto, A. Ryo, H. Hirano, Proteomic analysis of proteins related to prognosis of lung adenocarcinoma, Proteome Res. 13 (2014) 4686–4694.
[50] E. Klieser, R. Illig, S. Stattner, F. Primavesi, T. Jager, S. Swierczynski, T. Kiesslich, R. Kemmerling, C. Bollmann, P. Di Fazio, D. Neureiter, Endoplasmic reticulum stress in pancreatic neuroendocrine tumors is linked to clinicopathological parameters and possible epigenetic regulations, Anticancer Res. 35 (2015) 6127–6136.
[51] J.A. Schardt, D. Weber, M. Eyholzer, B.U. Mueller, T. Pabst, Activation of the unfolded protein response is associated with favorable prognosis in acute myeloid leukemia, Clin. Cancer Res. 15 (2009) 3834–3841.
[52] L. Bini, B. Magi, B. Marzocchi, F. Arcuri, S. Tripodi, M. Cintorino, J.C. Sanchez, S. Frutiger, G. Hughes, V. Pallini, D.F. Hochstrasser, P. Tosi, Protein expression profiles in human breast ductal carcinoma and histologically normal tissue, Electrophoresis 18 (1997) 2832–2841.
[53] S.V. Menezes, Z. Kovacevic, D.R. Richardson, The metastasis suppressor NDRG1 down-regulates the epidermal growth factor receptor via a lysosomal mechanism by up-regulating mitogen-inducible gene 6, J. Biol. Chem. 294 (2019) 4045–4064.
[54] K.W. Dunn, M.M. Kamocka, J.H. McDonald, A practical guide to evaluating colocalization in biological microscopy, Am. J. Physiol. Cell Physiol. 300 (2011) C723–C742.
[55] Y.C. Lu, W.C. Weng, H. Lee, Functional roles of calreticulin in cancer biology, Biomed. Res. Int. (2015) (2015) 526524.
[56] K. Salnikow, T. Kluz, M. Costa, Role of Ca(2+) in the regulation of nickel-inducible Cap43 gene expression, Toxicol. Appl. Pharmacol. 160 (1999) 127–132.
[57] O. Thastrup, A.P. Dawson, O. Scharff, B. Foder, P.J. Cullen, B.K. Drobak, P.J. Bjerrum, S.B. Christensen, M.R. Hanley, Thapsigargin, a novel molecular probe for studying intracellular calcium release and storage, Agents Actions 27 (1989) 17–23.
[58] A. Mattiazzi, E.G. Kranias, CaMKII regulation of phospholamban and SR Ca2+ load, Heart Rhythm. 8 (2011) 784–787.
[59] A.S. Leonard, I.A. Lim, D.E. Hemsworth, M.C. Horne, J.W. Hell, Calcium/calmodulin-dependent protein kinase II is associated with the N-methyl-D-aspartate receptor, Proc. Natl. Acad. Sci. U. S. A. 96 (1999) 3239–3244.
[60] H.P. Harding, Y. Zhang, A. Bertolotti, H. Zeng, D. Ron, Perk is essential for translational regulation and cell survival during the unfolded protein response, Mol. Cell 5 (2000) 897–904.
[61] H. Zinszner, M. Kuroda, X. Wang, N. Batchvarova, R.T. Lightfoot, H. Remotti, J.L. Stevens, D. Ron, CHOP is implicated in programmed cell death in response to impaired function of the endoplasmic reticulum, Genes Dev. 12 (1998) 982–995.
[62] T.E. Dever, Gene-specific regulation by general translation factors, Cell 108 (2002) 545–556.
[63] J.J. Chen, Regulation of protein synthesis by the heme-regulated eIF2alpha kinase: relevance to anemias, Blood 109 (2007) 2693–2699.
[64] T.E. Dever, J.J. Chen, G.N. Barber, A.M. Cigan, L. Feng, T.F. Donahue, I.M. London, M.G. Katze, A.G. Hinnebusch, Mammalian eukaryotic initiation factor 2 alpha kinases functionally substitute for GCN2 protein kinase in the GCN4 translational control mechanism of yeast, Proc. Natl. Acad. Sci. U. S. A. 90 (1993) 4616–4620.
[65] C. Hetz, F. Martinon, D. Rodriguez, L.H. Glimcher, The unfolded protein response: integrating stress signals through the stress sensor IRE1alpha, Physiol. Rev. 91 (2011) 1219–1243.
[66] D.T. Rutkowski, S.W. Kang, A.G. Goodman, J.L. Garrison, J. Taunton, M.G. Katze, R.J. Kaufman, R.S. Hegde, The role of p58IPK in protecting the stressed endoplasmic reticulum, Mol. Biol. Cell 18 (2007) 3681–3691.
[67] M. Hibi, A. Lin, T. Smeal, A. Minden, M. Karin, Identification of an oncoprotein- and UV-responsive protein kinase that binds and potentiates the c-Jun activation domain, Genes Dev. 7 (1993) 2135–2148.
[68] S. Gupta, T. Barrett, A.J. Whitmarsh, J. Cavanagh, H.K. Sluss, B. Derijard, R.J. Davis, Selective interaction of JNK protein kinase isoforms with transcription factors, EMBO J. 15 (1996) 2760–2770.
[69] J. Ye, R.B. Rawson, R. Komuro, X. Chen, U.P. Dave, R. Prywes, M.S. Brown, J.L. Goldstein, ER stress induces cleavage of membrane-bound ATF6 by the same proteases that process SREBPs, Mol. Cell 6 (2000) 1355–1364.
[70] H. Yoshida, T. Matsui, A. Yamamoto, T. Okada, K. Mori, XBP1 mRNA is induced by ATF6 and spliced by IRE1 in response to ER stress to produce a highly active transcription factor, Cell 107 (2001) 881–891.
[71] K. Lee, W. Tirasophon, X. Shen, M. Michalak, R. Prywes, T. Okada, H. Yoshida, K. Mori, R.J. Kaufman, IRE1-mediated unconventional mRNA splicing and S2P-mediated ATF6 cleavage merge to regulate XBP1 in signaling the unfolded protein response, Genes Dev. 16 (2002) 452–466.
[72] K.H. Tay, Q. Luan, A. Croft, C.C. Jiang, L. Jin, X.D. Zhang, H.Y. Tseng, Sustained IRE1 and ATF6 signaling is important for survival of melanoma cells undergoing ER stress, Cell. Signal. 26 (2014) 287–294.
[73] S.V. Menezes, S. Sahni, Z. Kovacevic, D.R. Richardson, Interplay of the iron-regulated metastasis suppressor NDRG1 with epidermal growth factor receptor (EGFR) and oncogenic signaling, J. Biol. Chem. 292 (2017) 12772–12782.
[74] Z. Kovacevic, D.R. Richardson, The metastasis suppressor, Ndrg-1: a new ally in the fight against cancer, Carcinogenesis 27 (2006) 2355–2366.
[75] Z. Kovacevic, S. Chikhani, D.B. Lovejoy, D.R. Richardson, Novel thiosemicarbazone iron chelators induce up-regulation and phosphorylation of the metastasis suppressor N-myc down-stream regulated gene 1: a new strategy for the treatment of pancreatic cancer, Mol. Pharmacol. 80 (2011) 598–609.
[76] W. Liu, F. Xing, M. Iiizumi-Gairani, H. Okuda, M. Watabe, S.K. Pai, P.R. Pandey, S. Hirota, A. Kobayashi, Y.Y. Mo, K. Fukuda, Y. Li, K. Watabe, N-myc downstream regulated gene 1 modulates Wnt-beta-catenin signalling and pleiotropically suppresses metastasis, EMBO Mol. Med. 4 (2012) 93–108.
[77] Z. Chen, J. Sun, T. Li, Y. Liu, S. Gao, X. Zhi, M. Zheng, Iron chelator-induced up-regulation of Ndrg1 inhibits proliferation and EMT process by targeting Wnt/beta-catenin pathway in colon cancer cells, Biochem. Biophys. Res. Commun. 506 (2018) 114–121.
[78] H.A. Askautrud, E. Gjernes, G. Gunnes, M. Sletten, D.T. Ross, A.L. Borresen-Dale, N. Iversen, M.A. Tranulis, E. Frengen, Global gene expression analysis reveals a link

between NDRG1 and vesicle transport, PLoS One 9 (2014) e87268.
[79] J.M. Timmins, L. Ozcan, T.A. Seimon, G. Li, C. Malagelada, J. Backs, T. Backs, R. Bassel-Duby, E.N. Olson, M.E. Anderson, I. Tabas, Calcium/calmodulin-dependent protein kinase II links ER stress with Fas and mitochondrial apoptosis pathways, J. Clin. Invest. 119 (2009) 2925–2941.
[80] P. Pinton, C. Giorgi, R. Siviero, E. Zecchini, R. Rizzuto, Calcium and apoptosis: ER-mitochondria Ca2+ transfer in the control of apoptosis, Oncogene 27 (2008) 6407–6418.
[81] D. Han, A.G. Lerner, L. Vande Walle, J.P. Upton, W. Xu, A. Hagen, B.J. Backes, S.A. Oakes, F.R. Papa, IRE1alpha kinase activation modes control alternate endoribonuclease outputs to determine divergent cell fates, Cell 138 (2009) 562–575.
[82] H. Mujcic, A. Nagelkerke, K.M. Rouschop, S. Chung, N. Chaudary, P.N. Span, B. Clarke, M. Milosevic, J. Sykes, R.P. Hill, M. Koritzinsky, B.G. Wouters, Hypoxic activation of the PERK/eIF2alpha arm of the unfolded protein response promotes metastasis through induction of LAMP3, Clin. Cancer Res. 19 (2013) 6126–6137.
[83] A. Nagelkerke, J. Bussink, H. Mujcic, B.G. Wouters, S. Lehmann, F.C. Sweep, P.N. Span, Hypoxia stimulates migration of breast cancer cells via the PERK/ATF4/LAMP3-arm of the unfolded protein response, Breast Cancer Res. 15 (2013) R2.
[84] Y.X. Feng, E.S. Sokol, C.A. Del Vecchio, S. Sanduja, J.H. Claessen, T.A. Proia, D.X. Jin, F. Reinhardt, H.L. Ploegh, Q. Wang, P.B. Gupta, Epithelial-to-mesenchymal transition activates PERK-eIF2alpha and sensitizes cells to endoplasmic reticulum stress, Cancer Discov. 4 (2014) 702–715.